Delft University of Technology

Document Version
Final published version

Citation (APA)
Sundman, B., Dupin, N., Sluiter, M. H. F., Fries, S. G., Guéneau, C., Hallstedt, B., Kattner, U. R., & Selleby, M. (2024). The Legacy of "The Regular Solution Model for Stoichiometric Phases and Ionic Melts". *Journal of Phase Equilibria and Diffusion*, *45*(6), 934-964. https://doi.org/10.1007/s11669-024-01163-2

Important note
To cite this publication, please use the final published version (if applicable).
Please check the document version above.

Copyright
In case the licence states "Dutch Copyright Act (Article 25fa)", this publication was made available Green Open Access via the TU Delft Institutional Repository pursuant to Dutch Copyright Act (Article 25fa, the Taverne amendment). This provision does not affect copyright ownership.
Unless copyright is transferred by contract or statute, it remains with the copyright holder.

Sharing and reuse
Other than for strictly personal use, it is not permitted to download, forward or distribute the text or part of it, without the consent of the author(s) and/or copyright holder(s), unless the work is under an open content license such as Creative Commons.

Takedown policy
Please contact us and provide details if you believe this document breaches copyrights.
We will remove access to the work immediately and investigate your claim.

This work is downloaded from Delft University of Technology.

Green Open Access added to TU Delft Institutional Repository

'You share, we take care!' - Taverne project

https://www.openaccess.nl/en/you-share-we-take-care

Otherwise as indicated in the copyright section: the publisher is the copyright holder of this work and the author uses the Dutch legislation to make this work public.

J. Phase Equilib. Diffus. (2024) 45:934–964
https://doi.org/10.1007/s11669-024-01163-2

REVIEW

The Legacy of "The Regular Solution Model for Stoichiometric Phases and Ionic Melts"

Bo Sundman[1] · Nathalie Dupin[2] · Marcel H. F. Sluiter[3,4] · Suzana G. Fries[5] · Christine Guéneau[6] · Bengt Hallstedt[7] · Ursula R. Kattner[8] · Malin Selleby[9]

Submitted: 24 July 2024 / in revised form: 18 September 2024 / Accepted: 18 October 2024 / Published online: 14 December 2024
© ASM International 2024

Abstract In 1970, Hillert and Staffansson published a paper entitled "The Regular Solution Model for Stoichiometric Phases and Ionic Melts". It was the beginning of the sublattice model that has been a key component in the development of Computational Thermodynamics. This formalism, now often called the Compound Energy Formalism (CEF), has been used to describe a great variety of phases driven by the need for accurate descriptions of thermodynamic phase stability in a wide range of materials involving many elements. The purpose of this paper is to describe the formalism, the physical meaning of its various parameters and the way they can be assessed using experimental and theoretical data. Furthermore, new developments derived from the CEF, such as the Effective Bond Energy Formalism, and other ideas for further development are presented.

Keywords Calphad · Gibbs energy · multicomponent · oxide systems · thermodynamic modeling · compound energy formalism · short range order

1 Introduction

Computational Thermodynamics (CT), first introduced as a method for the Calculation of Phase Diagrams (Calphad), is an integral part of materials science as it provides a practical framework for the modeling of phase stability, phase equilibria and phase transitions in materials. It requires highly accurate representations of the thermodynamic properties of all the relevant phases, both stable and metastable, as function of temperature and composition,

This invited article is part of a special tribute issue of the *Journal of Phase Equilibria and Diffusion* dedicated to the memory of Mats Hillert on the 100th anniversary of his birth. The issue was organized by Malin Selleby, John Ågren, and Greta Lindwall, KTH Royal Institute of Technology; Qing Chen, Thermo-Calc Software AB; Wei Xiong, University of Pittsburgh; and JPED Editor-in-Chief Ursula Kattner, National Institute of Standards and Technology (NIST).

✉ Marcel H. F. Sluiter
M.H.F.Sluiter@tudelft.nl

Bo Sundman
bo.sundman@gmail.com

1 OpenCalphad, Gif-sur-Yvette, France

2 Calcul Thermodynamique, Orcet, France

3 Materials Science and Engineering, Delft University of Technology, Delft, The Netherlands

4 Department of Materials Science and Engineering, Ghent University, Zwijnaarde, Belgium

5 Materials Research Department, Ruhr-University Bochum, Bochum, Germany

6 Service de Recherche en Corrosion et Comportement des Matériaux, CEA, Université Paris-Saclay, Gif-sur-Yvette, France

7 Institute for Materials Applications in Mechanical Engineering, RWTH Aachen University, Aachen, Germany

8 Materials Science and Engineering Division, National Institute of Standards and Technology, Gaithersburg, MD

9 Materials Science and Engineering, KTH Royal Institute of Technology, Stockholm, Sweden

and possibly pressure. CT relies on models describing the Gibbs energy of each phase in a multicomponent system and uses databases with model parameters assessed from experimentally measured and theoretically computed data for binary, ternary and, very rarely, higher-order systems.

J.W. Gibbs provided the theoretical foundations for the thermodynamic study of phase equilibria in his pioneering monograph "On the Equilibrium of Heterogeneous Substances".[1] Furthermore, Gibbs derived an important rule, the Gibbs phase rule, which dictates the number of phases that can co-exist in a mixture under certain conditions. Gibbs' work proved fertile soil for other researchers like van't Hoff who distilled useful approximate rules concerning the behavior of solutions. Prior experimentally observed relations, such as Henry's law, acquired a sound theoretical basis. Van Laar[2] was the first to utilize the theoretical framework, with a set of approximations which have come to be known as the 'regular-solution model', to produce an explicit mathematical description of phase equilibria in binary systems. His work produced prototype phase diagrams, which exhibited the most important general features of phase diagrams such as monotectic (-oid), eutectic (-oid) and peritectic (-oid) phase equilibria, retrograde solubility and immiscible solutions Unfortunately, this theoretical study went unrecognized until much later, when experimental studies for binary metallic systems showed its validity.

Parallel to these theoretical developments, experimentalists set out to determine phase diagrams. A pivotal role was played by the iron - carbon system. Sorby[3] and Roberts-Austen[4] performed experimental studies of phase equilibria in this system, but it was not until the turn of the century that the first reasonably complete, albeit inaccurate, phase diagram was published by Bakhuis Roozeboom.[5] Only several decades later a general agreed upon stable and metastable Fe-C diagram became available. The determination of this diagram revolutionized the understanding of tempered iron, the occurrence of grey and white cast iron and the hardenability and heat treatments of steel.

The enormous progress made in the understanding of Fe-C alloys inspired extensive experimental work on other systems to such an extent that, already in 1909 Jänecke[6] compiled a brief summary of binary and a few ternary systems. In the nineteen thirties well-known compendia of many binary systems could be assembled by Hansen[7,8] while some ternary systems were compiled by Jänecke.[9] The compendium by Hansen, entitled "Der Aufbau der Zweistofflegierungen: Eine kritische Zusammenfassung"[1][7,8] encouraged more theoretical work, such as described in the book "Thermodynamics of Alloys" by Wagner.[10]

[1] The structure of binary alloys: A critical summary.

The apparent basic validity of the regular-solution model motivated Meijering[11] to study precipitation and phase stability in binary Al-Cu alloys and before long multinary alloys were explored[12,13] as well. Kaufman investigated the effect of pressure in the Fe-Ni system.[14] He soon realized that a thermodynamic description was needed of pure elements in various crystal structures, that were not observed in reality for extrapolations in composition, temperature, and pressure.[14-16] In fact, van Laar[2] in 1908 already extrapolated properties of β brass towards pure Cu to obtain the melting point of hypothetical body-centered cubic (bcc) Cu. The requirement that the energy differences between various crystal structures of a particular element in the periodic table, the so-called "lattice stability", had to be the same for every binary or multinary that contained this particular element was clarified by Kaufman and Bernstein.[17] Expanding on this insight, that every binary in the limit towards a unary must have the same thermodynamic description, it was evident that every ternary in the limit to a particular binary must satisfy the same thermodynamic consistency. This made the thermodynamic description of the many binary and multinary phase diagrams a highly interlinked affair.[18,19] These efforts, initially by pen, paper and a ruler led to the birth of Calphad by Kaufman and Ansara in 1973.[20]

The regular solution model proved useful for a deeper physical understanding of other puzzling physical phenomena as well, such as spinodal decomposition. Hillert[21,22] showed that the periodic composition fluctuations experimentally observed in Cu-Ni-Fe alloys appeared naturally when an interfacial energy due to composition fluctuations was taken into account. This work was seminal to the subsequent Cahn-Hilliard description.[23]

In the regular solution model the energy of mixing is a parabolic function of composition. This function is symmetric with respect to the equiatomic composition and therefore gives rise to symmetric phase diagrams. As it was experimentally well established that most phase diagrams are not symmetric, a solution was found in the subregular solution model.[24]

A further component of the (sub)regular solution model is the configurational entropy. Complete random mixing is assumed which is not quite correct. Randomness occurs only when the energy of mixing is negligible relative to the thermal energy k_BT. The energy of mixing depends on the magnitude of interaction between the components of the mixture. When the pairwise interaction between the components is such that pairs of (un)like components are energetically favored, then minimization of the energy will naturally cause such pairs to be more abundant than they would be in a purely random solution. In the (sub)regular solution model the preference for (un)like pairs over the

random state is ignored. Therefore, the model entropy is overestimated and the energy contribution is less favorable than it is in reality. While these two factors partially counteract, it causes the (sub)regular solution model free energy (either Gibbs or Helmholtz) of the solid solution to be too unfavorable, particularly in concentrated solutions. Thus, too high critical temperatures are predicted for miscibility gaps. In the ordered state the neglect of partial disordering causes the (sub)regular solution model free energy to be too unfavorable too, especially in the vicinity of the transition temperature, but to a lesser degree than in the solid solution state. Therefore, the (sub)regular solution gives order–disorder transition temperatures that are too high.

Even in slightly more sophisticated models, such as those of Temkin[25] for ionic components and Gorsky-Bragg-Williams (GBW)[26-29] for lattice gases an exaggerated randomness is assumed. Thus, to improve the theoretical free energy, both energy and entropy need to be improved in tandem in the (sub)regular solution, in the Temkin, and in the GBW models.

Improvements to energy and entropy could be achieved by including correlations, defined as constituents not being perfectly randomly distributed with regard to one another. The quasi-chemical model[30] and the Bethe[31] approximation, both of which are based on the crude counting of the approximate number of configurations under constraints, yielded significant changes in phase diagrams. Kikuchi[32] found a systematic and consistent way to count configurations in the so-called cluster variation method (CVM).[33] From the seventies[34] onward this method has been used to compute topologically correct phase diagrams.[35] It even became possible to directly base the phase diagram calculations on the newly emerging first-principles total energy calculations[36] through the structure inversion method[37] based on perfectly ordered structures.[38-40] Still, the CVM was hard to apply to multinary alloys with non-trivial mixing behavior. Therefore, other more practical methods were needed. For this purpose, the compound energy formalism (CEF) of Hillert[41,42] has proven extremely effective. Initially, the energy contribution was formulated in terms of the typical regular solution mixing parameters that considered a mixed occupation on two sublattices. Its extension by Sundman and Ågren[43] to many sublattices and many constituents introduced the concept of "compound" which eventually gave birth to CEF. In this formulation[43] the CEF appears deceptively simple: the free energy is computed by summation of the contributions from these "compounds" and the randomly mixed configurational entropy terms of the distinct sublattices. Each of these sublattices has its own composition, the so-called 'site fractions', in the spirit of the GBW approximation for ordered phases, while simultaneously computing the energy term from the set of compounds corresponding to configurations where each sublattice is occupied by a single constituent that can be an element, a chemical species (possibly charged), or a vacancy. The CEF, unlike some other approaches, see e.g.,[44] yields a free energy function that allows the consideration of phase transitions. The energies of the compounds play a critical role, moreover they can be easily and routinely computed with first-principles density functional theory.[36] The CEF of Hillert,[41,42] as extended by Sundman and Ågren,[43] can therefore be regarded as a precursor to the structure inversion method.[37] The strength of the CEF is that it does not try to decompose the compound energies into cluster contributions such as in a cluster expansion,[45] or into regular solution mixing parameters such as in the conventional regular solution model. Such a decomposition into cluster contributions, while in principle accurate to any degree desired,[46] is not unique and can moreover give rise to spurious results if the set of compounds is too small to define all of the subcluster terms.[47]

However, the entropy description within the CEF has all the limitations of the usual Gorsky-Bragg-Williams approximation, such as giving too high transformation temperatures,[48] as already mentioned above. Therefore special efforts have been made to incorporate the effects of short range order (SRO), see section 3.2. The energy term can be made more accurate by selecting a larger supercell although only ordered structures that have periodicities that are commensurate with the selected supercell can be treated. Solid solutions and ordered superstructures are usually treated using small cells, e.g., face centred cubic (fcc) with 4 sublattices,[49,50] but it is entirely feasible to use a cell consisting of multiple conventional unit cells. Selecting larger cells, i.e., more sublattices has only a relatively minor impact on computational effort in CEF, quite unlike the case of the CVM[51-53] because the CEF uses the ideal configurational entropy approximation. The insight gained from cluster expansions that interactions associated with large numbers of sites contribute little to the energy can be gainfully employed to simplify the CEF and this yields the Effective Bond Energy Formalism,[54] discussed later in this article.

2 The Sublattice Model

In the early 1970s, Mats Hillert at the division of physical metallurgy, KTH Royal Institute of Technology, was engaged in developing tools for simulating phase transformation in steels. He had studied at the Massachusetts Institute of Technology and knew the early work of Kaufman[15] and was looking for a model for interstitial C in steels. Together with Staffansson, a professor in

metallurgy who knew the Temkin model[25] from his work with molten salts, Hillert adapted this model for interstitial solutions[41] using one sublattice for random mixing of the metals and the other one for the interstitial together with a vacancy constituent. The configurational entropy assumed random mixing of the metals on their sublattice and of the vacancies and the interstitials on the other.

Hillert knew that before one can simulate transformations in materials one must know how the equilibrium state changes with temperature and composition and his students started to develop a multicomponent thermodynamic database for steels using the sublattice (SL) model.[55-58] With a primitive assessment software they fitted model parameters to experimental data from their own work as well as from published data. At that time the computer facilities were very limited and each PhD student had to modify the software for each assessment and a calculation. It was not possible to combine the different assessments and develop a general software and database until the division managed to obtain its own minicomputer. The new software was based on a thermodynamic model[43] that generalized the sublattice model from 1970.[41] Each phase was modeled with one or more sublattices with one or more constituents in each sublattice and included a model for the ferromagnetic transition in Fe, Cr and Ni proposed by Inden.[59,60] The computational methods were also improved by a general algorithm for calculating equilibria published by Hillert[61] and implemented by Jansson[62] together with routines to calculate phase diagrams and an assessment module to fit model parameters to experimental data in a software, called Thermo-Calc[2].[63,64]

As the "sublattice model" was based on compounds (later called endmembers) it has also been called "compound energy model" and as it contains many models as special cases it was renamed "compound energy formalism" in 2001.[42] In this paper, we return to the original denomination "sublattice" because we will also consider the recent development of this formalism[54] keeping the main feature of the original formalism, i.e., its ideal entropy expression based on the sublattice fractions.

[2] Certain software packages are identified in this paper for proper reference. Such identification is not intended to imply recommendation or endorsement of any product or service by NIST or that the software identified are necessarily the best available for the purpose.

2.1 The Pure Elements, Unary Data

As already mentioned, Kaufman et al.[15,65] introduced lattice stabilities defined as the difference in Gibbs energy between the metastable and the stable allotrope for an element A

$$^{\circ}G_{\mathrm{A}}^{\mathrm{meta}}(T) -^{\circ} G_{\mathrm{A}}^{\mathrm{stab}}(T) = a - bT \qquad \text{(Eq 1)}$$

Kaufman used this to model phase diagrams of many systems. However, no heat capacity was modeled in this first generation description of the elements. In the second generation of the element descriptions presented in section 2.1.1, this shortcoming was addressed, i.e., the heat capacities were added and this generation is still used in most databases. The emerging third generation of descriptions addressing issues in the second generation will be presented in section 2.1.2.

2.1.1 The 2nd Generation Descriptions of the Elements

The Scientific Group Thermodata Europe (SGTE) started working on a new unary database at the beginning of the 1980s in which heat capacities were added to all elements. This compilation of 78 elements was eventually published by Dinsdale in 1991.[66] The reference used was the enthalpy at 298.15 K and the entropy at 0 K, both at 1 bar, for the most stable state of each element. An exception was made for the elements with magnetic transitions for which the reference state is a hypothetical paramagnetic state because the magnetic Gibbs energy is added separately as explained below. The reference state is called SER, the Standard Element Reference. Since the entropy at 0 K is given the value zero, this reference state is usually denoted $H_{\mathrm{A}}^{\mathrm{SER}}$. The Gibbs energy of the most stable state given relative to this reference is:

$$^{\circ}G_{\mathrm{A}}^{\mathrm{SER}}(T) - H_{\mathrm{A}}^{\mathrm{SER}}(298) = a + bT + cT\ln(T) + \sum_{n} d_n T^n \qquad \text{(Eq 2)}$$

where a, b, c, d_n are the model parameters fitted to experimental information, most importantly the heat capacity. In Fig. 1(a), (b), and (c) the Gibbs energy functions of Fe for fcc, hexagonal close packed (hcp) and liquid relative to the bcc phase are shown. The fact that bcc is stable at low T for Fe is due to the heat capacity contribution from the ferromagnetic transition.

If an element has a magnetic transition in a phase the situation is more complicated because a detailed modeling of the magnetic transition was, and still is, a complex problem in physics. But within the Calphad community a numerical fit to the general shape of the magnetic contribution to the heat capacity proposed by Inden[59,60] was adopted. This was based on the heat capacity curves for Co,

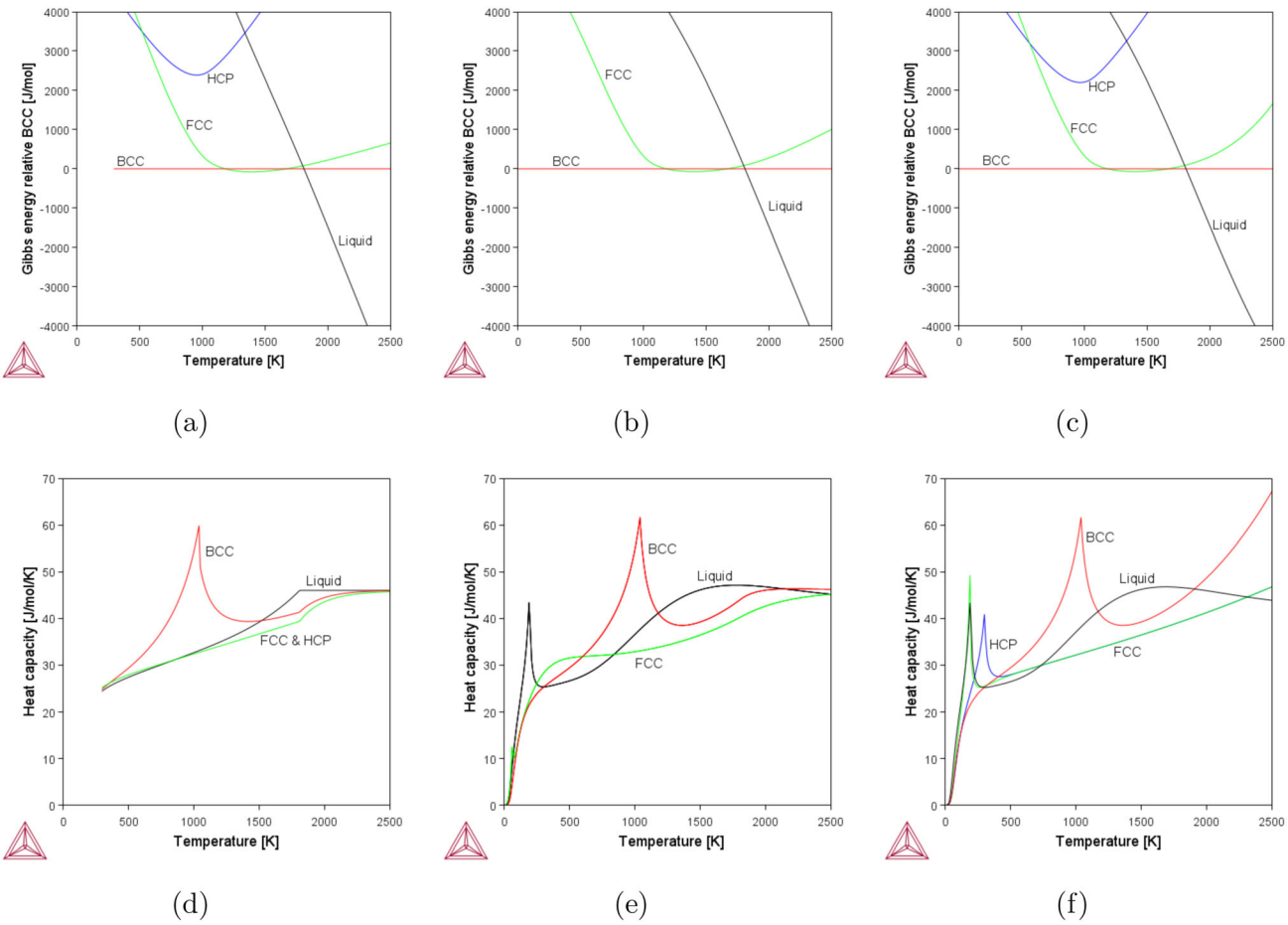

Fig. 1 In (a), (b) and (c) the calculated molar Gibbs energy of pure Fe phases relative to the bcc phase is plotted vs temperature for three different unary datasets: in (a) the 1991 unary[66] (which has no data below 298.15 K), (b) an evaluation by Chen and Sundman[69] and, (c) the current 3rd generation database by He et al.[70] In (a) and (c) the Gibbs energy for the hcp phase is also included. In (d), (e) and (f) the heat capacity for pure Fe phases is plotted vs temperature for the same datasets. In (e) from[69] and in (f) from[70] the heat capacity is zero at $T = 0$ K. In (f) the extrapolation of the heat capacities for the solid phases to high temperatures is not restricted due to the EEC, see the text for explanations

Fe and Ni and was slightly modified/simplified by Hillert and Jarl[67] and implemented in the Thermo-Calc software by Hertzman and Sundman[58] in their assessment of Fe-Cr. In Fig. 1(d), (e), and (f) the heat capacity curve for the bcc phase indicates the significant contribution from the ferromagnetic transition at 1043 K.

In the magnetic model the contribution to Gibbs energy for a phase α, ${}^{\mathrm{mgn}}G_m^{\alpha}$, depends on two magnetic properties: the Bohr magneton number, β^{α}, and the Curie temperature, T_C^{α}

$$ {}^{\mathrm{mgn}}G_m^{\alpha} = RTf(\tau)\ln(\beta^{\alpha}+1) \quad \text{(Eq 3)} $$

$$ \tau = T/T_C^{\alpha} \quad \text{(Eq 4)} $$

where $f(\tau)$ is a general function fitted to the integrated heat capacity contribution by Hillert and Jarl.[67]

The successful work on the steel database at KTH[68] convinced SGTE that a separate magnetic contribution should be included in its unary database. In particular parameters for β and T_C should be provided. For a non-magnetic element A, $\beta_{\mathrm{A}} = 0$, $T_{CA} = 0$ and ${}^{\mathrm{mgn}}G_m = 0$. Since the magnetic contribution is added separately, the reference state for magnetic allotropes in the SGTE unary database represents a hypothetical paramagnetic state.

The 1991 unary compilation[66] was a big success and has been used worldwide as a basis to assess thermodynamic model parameters for materials. A common ground for the elements made it possible to combine thermodynamic descriptions from different groups and thereby accelerate the collaborative work on multicomponent databases.

Using expressions like Eq 2 meant that one had to take care of the extrapolations in temperature outside the stable range of the reference phase as high heat capacities may make the solid phase stable again at high temperatures. Thus breakpoints were introduced in the 1991 SGTE

unary database at the melting temperature of the solid reference phase and the heat capacity of the extrapolated solid was forced to approach that of the liquid above the melting temperature and vice versa for the liquid, see Fig. 1(d). This is usually referred to as "the SGTE extrapolation".

2.1.2 The 3rd Generation Descriptions of the Elements

Already at the Ringberg workshop in 1995[71] suggestions were put forward to improve the descriptions of the 1991 unaries and make them more physically sound. One problem with the SGTE extrapolation is that there will be kinks in the heat capacity at the melting temperature of the constituent elements of any compound or endmember that is based on the Kopp-Neumann rule,[72] see Eq 19. The first attempt to make use of the recommendations from the Ringberg workshop was the reassessment of pure iron by Chen and Sundman in 2001,[69] see Fig. 1(b) where the molar Gibbs energy for bcc, fcc, and liquid Fe is plotted and the corresponding heat capacity in Fig. 1(e). The concept of the first and second generation of functions for the temperature dependence was introduced by Kaufman and Ågren[73] and the descriptions of the unaries from 1991 were considered to belong to the second generation. The paper by Chen and Sundman laid the foundation for an international effort to develop models for the next generation, the 3rd, of Calphad models. They described the heat capacity for a solid element as

$$C_P = 3R\left(\frac{\theta_E}{T}\right)^2 \frac{\exp(\frac{\theta_E}{T})}{\exp(\frac{\theta_E}{T}-1)} + aT + bT^n \qquad \text{(Eq 5)}$$

where the first term is the contribution from the harmonic lattice vibrations and θ_E (K) is the Einstein temperature. The second term is the contribution from the electronic excitation and low-order anharmonic lattice vibration effects such as the correction from C_V to C_P associated with thermal volume expansion. The third term is the contribution from the high-order anharmonic lattice vibration effects. This expression is used in the 3rd generation and the expression for the corresponding Gibbs energy for an element A is

$$^{\circ}G_A - H_A^{SER}(298) = E_0 + \frac{3}{2}R\theta_E + 3RT\ln\left[1-\exp(-\frac{\theta_E}{T})\right] - \frac{a}{2}T^2 - \frac{b}{n(n+1)}T^{n+1} \qquad \text{(Eq 6)}$$

where E_0 denotes the cohesive energy (total energy excluding the vibrational contribution) at 0 K and the second term is the contribution from the zero point energy to the Gibbs energy.

In the 3rd generation, the liquid phase is described using the two-state model[74,75] in which all atoms in the liquid are either in a translational state or a vibrational state. With this model only one temperature range is used and no artificial break point is needed at the melting temperature.

A single temperature range was also suggested for solid phases[70,76] and for this purpose, the Equal Entropy Criterion (EEC)[77] was proposed which simply states that any solid phase with a higher molar entropy than that of a stable liquid must not be allowed to participate in an equilibrium, such a solid should simply be ignored by the software. The treatment has been criticized[78] partly because EEC means the thermodynamic software must perform such checks while calculating the equilibrium and partly because the extrapolated heat capacity will sometimes reach very high values at elevated temperatures. To remedy this, a second expression could be introduced for temperature ranges above the melting temperature. In a work on pure Al[79] it was found that an "instability temperature" above which the solid can no longer exist occurred around 200 K above the melting temperature for fcc-Al. Such an "instability temperature" could be scaled to the melting temperature of an element. However, the best solution to this high temperature issue is yet to be found.

In the 3rd generation description, the magnetic model has been improved, first in the paper by Chen and Sundman[69] in which they carefully investigated the magnetic and paramagnetic part of the heat capacity of bcc-Fe and refined the model developed by Hillert and Jarl[67] that was based on the model by Inden.[59] Later a revised magnetic model was presented by Xiong et al.[80] in which each magnetic phase was assigned both a Curie temperature and a Néel temperature. These improvements mainly affect binary and higher-order systems for which the so-called effective magnetic moment was introduced.

The work on the 3rd generation models and descriptions has resulted in a number of doctoral theses and papers and references to these can be found in a paper entitled "Third generation Calphad for elements - model discussion with hands-on instructions and examples"[81] published in the same journal issue.

2.2 Composition Variables in a Thermodynamic System

In this paper the terms atom, element or component will be used for the basic composition variables according the Gibbs phase rule that the degrees of freedom of a system is:

$$f = n + 2 - p \quad \text{(Eq 7)}$$

where f is the number of degrees of freedom, n is the number of components (in this section denoted by capital letters A, B, C $\cdots$), the number "2" represents the intensive variables temperature (T) and pressure (P) and (lower case) p is the number of prescribed stable phases. In order to calculate the equilibrium for a system, f is the number of external conditions to be set. A thermodynamic system normally has several phases and each phase is modeled independently. Many crystalline phases have different sets of sites and the sublattice notation can be used even if there is a single set of sites (or no sites at all as for the gas phase). A model for a phase with 2 sublattices can be denoted:

$$(r, s, t)_{a_1}(u, v, w)_{a_2} \quad \text{(Eq 8)}$$

where the parenthesis around the constituents r, s, t define a sublattice and the indices a_j denote the number of sites on the sublattice j. In most cases, the constituents are the same as the components but, for example, in the gas phase there can be molecules, or species, with two or more components with fixed stoichiometric factors, for example, H_2O. Such chemical species can be used as constituents in any phase. Frequently a phase has more constituents than there are components in the system.

The sublattices are related to the crystallographic structure but simplifications have often been made due to computer limitations or lack of data. A phase with no sublattices has just a single set of sites, normally with $a_1 = 1$.

The sum of the constituent fractions, denoted $y_i^{(s)}$, on any sublattice s is unity:

$$\sum_i y_i^{(s)} = 1 \quad \text{(Eq 9)}$$

where the parenthesis around s is used to avoid confusion with a power but in some cases other notations are used. For example, the Wyckoff symbol of the site corresponding to the sublattice is sometime used. The notations $'$, $''$ are often used for the first and second sublattice when there only 2, but superscript (s), $s = 1, 2, \cdots$ is preferred when there are more than two sublattices.

The configurational entropy is zero when there is a single constituent in each sublattice. This is the idea of the Temkin model and it means the Gibbs energy for such a case has the same meaning as for a pure element in a solution phase with a single set of sites. An endmember has a single constituent in each sublattice. The same species can be a constituent in several sublattices, for example, to describe ordering.

The fact that the species of a phase can be different from the components of the system means that the number of moles of a component A in a phase for one formula unit of the phase and its mole fraction must be calculated from the site fractions by:

$$N_A = \sum_s a_s \sum_i b_{iA} y_i^{(s)} \quad \text{(Eq 10)}$$

$$x_A = \frac{N_A}{\sum_B N_B} \quad \text{(Eq 11)}$$

where b_{iA} is the stoichiometric factor of component A in the species i. The factor b_{iA} is zero if component A is not part of constituent i and unity if i is A. The species i may include two or more components. For example, if i represents the species "$FeO_{1.5}$" then $b_{iFe} = 1$ and $b_{iO} = 1.5$. In Eq 11 for the mole fraction of A, the sum over B is for all components.

A second set of constituent fractions, see section 3.3, calculated from the basic set of site fractions, $y_i^{(s)}$, can be used for the composition dependence of model parameters which describe the disordered state of a phase.

2.3 The Model

2.3.1 The Gibbs Energy of a Phase

The Gibbs energy per mole of formula unit of a phase described with the sublattice model is:

$$G_M = {}^{\text{srf}}G_M - T\,{}^{\text{cfg}}S_M + {}^{\text{phy}}G_M + {}^{\text{E}}G_M \quad \text{(Eq 12)}$$

where ${}^{\text{srf}}G_M$ is the surface of reference of the phase, T the absolute temperature, ${}^{\text{cfg}}S_M$ the configurational entropy, ${}^{\text{phy}}G_M$ contributions from a physical model, such as the magnetic model, and finally ${}^{\text{E}}G_M$ the excess Gibbs energy. The subscript "M" rather than "m", as used in Eq 12, indicates that the equation is for one mole of formula units, not one mole of atoms. The number of atoms A, N_A, in one formula unit of the phase is given by Eq 10 and the mole fraction x_A by Eq 11.

The expression for the Gibbs surface of reference, ${}^{\text{srf}}G_M$ is:

$${}^{\text{srf}}G_M = \sum_I P_I(Y)\,{}^{\circ}G_I \quad \text{(Eq 13)}$$

where I is an endmember specifying a constituent i in each sublattice, $P_I(Y)$ is the product of one constituent fractions $y_i^{(s)}$ for each sublattice s as specified by the endmember I

and $^{\circ}G_I$ is the Gibbs energy of the endmember I in this phase.

$P_I(Y)$ can also be interpreted as a probability of the endmember I. The Gibbs energy of an endmember of phase α with an explicit set of constituents is denoted $^{\circ}G^{\alpha}_{\mathrm{Fe:Cr:Ni}}$ where the colon separates the Fe, Cr, Ni constituents in the different sublattices.

The configurational entropy, $^{\mathrm{cfg}}S_M$, assumes ideal mixing of the constituents on each sublattice and is given by:

$$^{\mathrm{cfg}}S_M = -R\sum_s a_s \sum_i y_i^{(s)} \ln y_i^{(s)} \qquad \text{(Eq 14)}$$

where a_s is the number of sites on sublattice s.

Most models for specific physical contributions to the Gibbs energy, for example, the magnetic model in Eq 3, express this contribution per mole of atoms whereas in Eq 12 it should be per mole formula unit. Thus one must multiply with the number of atoms in the formula unit of the phase:

$$^{\mathrm{phy}}G_M = N\ ^{\mathrm{phy}}G_m \qquad \text{(Eq 15)}$$

where N is the moles of atoms per formula unit of the phase. In the early use of the sublattice model it was not realized that the Gibbs energy was defined per mole formula units whereas $^{\mathrm{phy}}G_m$ in the magnetic model was per mole of atoms. For example, this was the case for the magnetite phase in Fe-O,[82] but the mistake was compensated by using an unrealistic Bohr magneton number as pointed out by Ref 83.

The physical models, such as the magnetic model mentioned above, normally depend on properties that vary with the composition, for example, the Curie temperature and the Bohr magneton number. This composition dependence is described by endmember and excess parameters in the same way as the Gibbs energy. Each of these properties must have a unique identifier and may depend on composition, and possibly temperature and pressure.

$^{\mathrm{E}}G_M$ is the excess Gibbs energy allowing to take into account the interaction between constituents that are present together:

$$^{\mathrm{E}}G_M = \sum_J P_J(Y)\ L_J(Y) \qquad \text{(Eq 16)}$$

where J is a constituent array with two or more constituents in at least one sublattice. $P_J(Y)$ is the product of the fractions of these constituents and expressions for $L_J(Y)$ can be found in sections 2.3.3 to 2.3.5.

All of the parameters in Eq 12 can depend on the pressure, P, but for calculations at high pressures special models must be used to avoid non-physical extrapolations, see for example Lu et al.[84]

In this paper we will only consider the modeling of the Gibbs energy and physical models which contribute to the Gibbs energy but the same kind of equations with model parameters which depend on temperature, pressure and the constitution can be used to describe other properties that are related to the phase, for example, atomic mobility, viscosity, resistivity. In several commercial databases many such properties are available.

2.3.2 Endmember Parameters for a Phase

In the sublattice model the phases have endmembers with several constituents in the different sublattices. A phase β with with 2 sublattices and 2 elements in each can be denoted:

$$(\mathrm{A},\mathrm{B})_{a_1}(\mathrm{A},\mathrm{C})_{a_2} \qquad \text{(Eq 17)}$$

assuming A and B mix in the first sublattice with a_1 sites and A and C mix in the second sublattice with a_2 sites. The Gibbs energies of the endmembers $\mathrm{A}_{a_1}\mathrm{A}_{a_2}$ (A:A) and $\mathrm{A}_{a_1}\mathrm{C}_{a_2}$ (A:C) can be written:

$$^{\circ}G^{\beta}_{\mathrm{A:A}} - (a_1+a_2)H^{\mathrm{SER}}_{\mathrm{A}} = g^{\beta}_{\mathrm{A:A}} + (a_1+a_2)\ ^{\circ}G^{\mathrm{SER}}_{\mathrm{A}} \qquad \text{(Eq 18)}$$

$$^{\circ}G^{\beta}_{\mathrm{A:C}} - a_1H^{\mathrm{SER}}_{\mathrm{A}} - a_2H^{\mathrm{SER}}_{\mathrm{C}} = g^{\beta}_{\mathrm{A:C}} + a_1\ ^{\circ}G^{\mathrm{SER}}_{\mathrm{A}} + a_2\ ^{\circ}G^{\mathrm{SER}}_{\mathrm{C}} \qquad \text{(Eq 19)}$$

where $^{\circ}G^{\mathrm{SER}}_{\mathrm{A}}$ and $^{\circ}G^{\mathrm{SER}}_{\mathrm{C}}$ are from Eq 2 in the unary database. The term $g^{\beta}_{\mathrm{A:A}}$ normally is a linear expression in T which means the phase β for pure A has the same heat capacity as the reference phase for element A. If β is stable for pure A this parameter should be part of the unary database. If the phase β is magnetic the magnetic contribution is added separately. If a sublattice constituent is not a pure element, the reference state for each element forming this constituent must be taken into account.

$^{\circ}G^{\beta}_{\mathrm{A:C}}$ represents the Gibbs energy of a compound and if $g^{\beta}_{\mathrm{A:C}}$ is constant or depends linearly on T, the heat capacity of this compound is a weighted average of the heat capacities of the elements which is known as the Kopp-Neumann rule.[72] Higher order powers of T in $g^{\beta}_{\mathrm{A:C}}$ can create problems with extrapolations. If $^{\circ}G^{\beta}_{\mathrm{A:C}}$ is the Gibbs energy of a stable compound it can be evaluated from experimental data. But together with the 3rd generation unary one must take care that the heat capacity (and the entropy if the compound is perfectly crystalline) is zero at $T = 0$ K.

The bond energies between constituents in different sublattices are described by the endmembers. In the next sections, the excess parameters model interactions between

constituents in the same sublattice for binary, ${}^{E.\mathrm{bin}}G_M$, and ternary, ${}^{E.\mathrm{ter}}G_M$, systems. Simultaneous interaction between two constituents in two sublattices can be taken into account as described in section 2.3.5.

2.3.3 Binary Excess Parameters

The variation of the bond energies between the constituents within a sublattice is described by the excess parameters, see for example Hillert.[85] For a binary system the Redlich-Kister (RK) series [86] is the most commonly used. For the sake of simplicity this is illustrated here for a phase with only one sublattice where the site fractions, $y_i^{(s)}$ are the same as the molar fractions, x_i. For a substitutional multicomponent system this gives the excess term:

$$ {}^{E.\mathrm{bin}}G_M = \sum_i \sum_{j>i} x_i\, x_j \sum_{v=0}^{n} (x_i - x_j)^v \;\; {}^{v}L_{i,j} \qquad \text{(Eq 20)} $$

where the parameters ${}^{v}L_{i,j}$ can be constants or depend linearly on T. Higher order powers of T must be used with care and only if there is excess heat capacity data. The index v is called the degree of the parameter, and from experience a higher degree than 3 should not be used. Each sublattice can have such excess parameters using site fractions instead of mole fractions as discussed in section 2.5.3.

2.3.4 Higher Order Excess Parameters

In ternary and higher order systems, it is possible to use interactions represented by parameter multiplied with the mole fractions. For a ternary substitutional system:

$$ {}^{E.\mathrm{ter}}G_M = \sum_i \sum_{j>i} \sum_{k>j} x_i\, x_j\, x_k\, L_{i,j,k} \qquad \text{(Eq 21)} $$

and in case a single parameter is not sufficient in a ternary system, Hillert[85] introduced a composition dependence which extrapolates symmetrically to higher order systems and also discusses other ternary extrapolation methods. Quaternary or higher order interactions are rare and never composition dependent.

2.3.5 Sublattices and Excess Model Parameters

For a phase with sublattices, the excess equations in sections 2.3.3 and 2.3.4 can be used independently on each sublattice using the site fractions $y_i^{(s)}$ instead of the mole fractions, x_i as shown also in sections 2.5.2 and 2.5.3. The constituents in different sublattices are separated by a colon (as in the endmembers) and the interacting constituents in the same sublattice are separated by a comma.

A model parameter usually depends on the constituents in all sublattices but in order to indicate that a parameter (endmember or excess) does not depend on the constituents in a specific sublattice, an asterisk, "*", can be used for this sublattice in the set of constitutents. This is also known as a "wildcard" and can be useful when there is a lack of experimental or theoretical data or when generalizing a model for a specific phase, see section 2.5.4.b, 3.4 and 3.5.

For phases with sublattices there is an additional important excess parameter related to the so called reciprocal reaction between 2 constituents in 2 different sublattices, i.e., $(\mathrm{A,B})_{\mathrm{a}_1}(\mathrm{C,D})_{\mathrm{a}_2}$. Considering the following reaction:

$$ \mathrm{A}_{\mathrm{a}_1}\mathrm{C}_{\mathrm{a}_2} + \mathrm{B}_{\mathrm{a}_1}\mathrm{D}_{\mathrm{a}_2} = \mathrm{A}_{\mathrm{a}_1}\mathrm{D}_{\mathrm{a}_2} + \mathrm{B}_{\mathrm{a}_1}\mathrm{C}_{\mathrm{a}_2} \qquad \text{(Eq 22)} $$

one can define the Gibbs energy:

$$ \Delta G_{\mathrm{AB:CD}} = {}^{\circ}G_{\mathrm{A}_{\mathrm{a}_1}\mathrm{D}_{\mathrm{a}_2}} + {}^{\circ}G_{\mathrm{B}_{\mathrm{a}_1}\mathrm{C}_{\mathrm{a}_2}} - {}^{\circ}G_{\mathrm{A}_{\mathrm{a}_1}\mathrm{C}_{\mathrm{a}_2}} - {}^{\circ}G_{\mathrm{B}_{\mathrm{a}_1}\mathrm{D}_{\mathrm{a}_2}} \qquad \text{(Eq 23)} $$

If the absolute value of $\Delta G_{\mathrm{AB:CD}}$ is large, this can create a miscibility gap[87] which can be suppressed or decreased using a reciprocal parameter $L_{\mathrm{A,B:C,D}}$ which is multiplied with all 4 constituent fractions. The corresponding contribution to the excess term is thus the following:

$$ {}^{E.\mathrm{rcp}}G_M = y_{\mathrm{A}}^{(1)}\, y_{\mathrm{B}}^{(1)}\, y_{\mathrm{C}}^{(2)}\, y_{\mathrm{D}}^{(2)}\, L_{\mathrm{A,B:C,D}} \qquad \text{(Eq 24)} $$

If a phase has several sublattices and constituents it means there are many such reciprocal reactions.

The reciprocal parameter is important and discussed in section 3.1 for liquids and in section 3.2 where it is used to describe SRO in phases with order–disorder transitions. The excess Gibbs energy for a phase with several sublattices and constituents is thus a sum of several contributions:

$$ {}^{\mathrm{E}}G_M = {}^{E.\mathrm{bin}}G_M + {}^{E.\mathrm{ter}}G_M + {}^{E.\mathrm{rcp}}G_M \qquad \text{(Eq 25)} $$

where the model parameters come from several independently assessed systems.

2.4 The Chemical Potentials of the Endmembers of a Phase

An important thermodynamic property is the chemical potential, denoted μ_i, for the component i in a system. The chemical potential for component i is defined as:

$$ \mu_i = \left(\frac{\partial G}{\partial N_i}\right)_{T,P,N_{j\neq i}} \qquad \text{(Eq 26)} $$

where the values of T, P and the amounts of all other components, N_j, are kept constant.

The chemical potentials for a phase can be calculated from its Gibbs energy model and at equilibrium, when the Gibbs energy is at a minimum, the chemical potentials of the components must be the same in all stable phases. But as the models are defined using fractions (mole, mass or site) and phases sometimes have other constituents than the

components, Eq 26 cannot be used directly for a particular phase. But for any phase α with or without sublattices we can always calculate the chemical potential of an endmember, I, i.e., by specifying a single constituent in each sublattice. As the amount of any other constituent must be constant, the equation is:

$$\mu_I^\alpha = G_M^\alpha + \sum_s \left(\frac{\partial G_M^\alpha}{\partial y_{i\in I}^{(s)}}\right)_{T,P,y_{j\neq i}} - \sum_s \sum_j y_j^{(s)} \left(\frac{\partial G_M^\alpha}{\partial y_j^{(s)}}\right)_{T,P,y_{k\neq j}} \quad \text{(Eq 27)}$$

as derived by Sundman and Ågren.[43]

For example, in the system Fe-Cr-C, in the ferrite phase, modeled as $(Cr,Fe)_1(C,Va)_3$, one can use Eq 27 to calculate the chemical potentials for two endmembers sharing the same species in all sublattices but one:

$$\mu_{Fe:C} = G_M + \frac{\partial G_M}{\partial y_{Fe}} + \frac{\partial G_M}{\partial y_C} - \left(y_{Fe}\frac{\partial G_M}{\partial y_{Fe}} + y_{Cr}\frac{\partial G_M}{\partial y_{Cr}} + y_C\frac{\partial G_M}{\partial y_C} + y_{Va}\frac{\partial G_M}{\partial y_{Va}}\right) \quad \text{(Eq 28)}$$

$$\mu_{Fe:Va} = G_M + \frac{\partial G_M}{\partial y_{Fe}} + \frac{\partial G_M}{\partial y_{Va}} - \left(y_{Fe}\frac{\partial G_M}{\partial y_{Fe}} + y_{Cr}\frac{\partial G_M}{\partial y_{Cr}} + y_C\frac{\partial G_M}{\partial y_C} + y_{Va}\frac{\partial G_M}{\partial y_{Va}}\right) \quad \text{(Eq 29)}$$

where the indication of sublattice superscripts and what is kept constant have been omitted for clarity. At equilibrium the chemical potentials of the endmembers are the sum of the chemical potentials of the individual constituents:

$$\mu_{Fe:Va} = \mu_{Fe} + 3\mu_{Va} \quad \text{(Eq 30)}$$

$$\mu_{Fe:C} = \mu_{Fe} + 3\mu_C \quad \text{(Eq 31)}$$

where the factor 3 comes from the number of interstitial sites in the bcc structure. At equilibrium the chemical potential of Va is zero and the chemical potential of C becomes:

$$\mu_C = \frac{1}{3}(\mu_{Fe:C} - \mu_{Fe:Va}) = \frac{1}{3}\left[\left(\frac{\partial G_M}{\partial y_C}\right)_{T,P,y_{i\neq C}} - \left(\frac{\partial G_M}{\partial y_{Va}}\right)_{T,P,y_{i\neq Va}}\right] \quad \text{(Eq 32)}$$

where all identical partial derivatives in Eq 28 and 29 have been eliminated. It is obvious that the chemical potential of C is independent of the endmember constituent in the first sublattice. If a constituent is a stoichiometric combination of several components, one can again use relations such as Eq 30 to obtain the chemical potential of each one. If a component is part of several constituents of a phase, at equilibrium it must have the same chemical potential in all of them.

A popular algorithm to calculate the equilibrium of a system is based on equating the chemical potentials of all components in all stable phases. There are cases when the sublattice model used for a phase makes it impossible to obtain explicitly the chemical potentials for a component but this is not necessary for calculating the equilibrium using the algorithm proposed by Hillert.[61] Further details on how to implement and use this algorithm are discussed by Jansson[62] and Sundman et al.[88]

2.5 Application to Various Cases

This section will present different cases of the sublattice model. It will allow to rewrite some of the rather complex equations presented in sections 2.2 and 2.3 in simpler form.

2.5.1 Substitutional Solutions

As discussed in the introduction, the modeling of substitutional solutions started well before the introduction of the sublattice model. However, this rather simple case is also a particular case of this complex model when only one single sublattice is considered. According to Eq 11 the site fractions are then identical to the molar fractions of the phase. The different contributions of Eq 12 are simply expressed as follows.

$${}^{srf}G_M = \sum_i x_i\, {}^\circ G_i \quad \text{(Eq 33)}$$

$${}^{cfg}S_M = -R\sum_i x_i \ln x_i \quad \text{(Eq 34)}$$

$${}^{E}G_M = \sum_i \sum_{j>i} \sum_v x_i\, x_j\, (x_i - x_j)^v\, {}^vL_{i,j} + \sum_i \sum_{j>i} \sum_{k>j} x_i\, x_j\, x_k\, L_{i,j,k} \quad \text{(Eq 35)}$$

The meaning of the parameters ${}^\circ G_i$, representing the descriptions of the pure elements, has been discussed in section 2.1. The different contributions of the excess term, ${}^EG_M$, were discussed in sections 2.3.3 and 2.3.4 representing the binary and ternary excess parameters, respectively. Given that the descriptions for the elements are fixed, these parameters are assessed to fit the experimental knowledge on the thermodynamic properties of the solution phase and its equilibria with other phases in the system. Results from First-Principles (FP) calculations, such as those employing Special Quasi-random Structures,[89] may help in the parameter assessment of metastable solutions, or when no experimental data are available. In order to properly describe multicomponent systems, it is important to assess these interactions for all the solution phases of the constituting binary systems. This includes the description of the stable and metastable composition and temperature ranges.

2.5.2 Stoichiometric Compounds

A stoichiometric compound can also be considered as a special case of the sublattice formalism when there is only one constituent in each of the sublattices. The configurational entropy as well as the excess Gibbs energy term is then zero.

Actually, Hillert and Staffansson[41] have used a slightly different definition for stoichiometric phases where each element is present in only one sublattice. The ternary extension of a binary stoichiometric compound $(A)_a(B)_b$ is then also considered a stoichiometric phase if C enters in either the first sublattice following the model $(A,C)_a(B)_b$ or in the second $(A)_a(B,C)_b$. Therefore, this kind of phase is sometimes called semi-stoichiometric. The relationship between composition and sublattice fraction is then very simple. When no vacancies are considered, it is just $x_i = a_i y_i/(a+b)$ where a_i is the multiplicity of the sublattice hosting i.

This model has been used for many phases and in particular to model the extension of binary carbides into ternary systems using the model $(A,B)_a(C)_b$,[90-95] to cite only a few early studies. The different terms of the Gibbs energy of such a phase is then expressed as follows:

$$^{\mathrm{srf}}G_M = \sum_i y_i \, {}^{\circ}G_{i:\mathrm{C}} \qquad \text{(Eq 36)}$$

$$^{\mathrm{cfg}}S_M = -\, a R \sum_i y_i \ln y_i \qquad \text{(Eq 37)}$$

$$^{\mathrm{E}}G_M = \sum_i \sum_{j>i} \sum_v y_i \, y_j \, (y_i - y_j)^v \, {}^{v}L_{i,j:\mathrm{C}} \qquad \text{(Eq 38)}$$

When applied to a ternary system, the model is defined along a line between two binary endmembers, A_aC_b and B_aC_b. Often only one endmember is stable and can be experimentally studied. The other one can be assessed from experimental knowledge of the extension of the composition range of the phase together with the excess parameters. The expressions discussed in section 2.1 are used to assess the Gibbs energy of the compounds. Nowadays, FP results can help to better estimate such parameters.

Equation 38 is similar to Eq 20 but uses the site fraction rather than the overall composition as variable. The expression given here allows to consider more than two elements in the first sublattice.

2.5.3 Interstitial Solutions

Interstitial solutions have already been mentioned in previous sections and are here discussed in greater detail. This case differs from the previous substitutional solutions as vacancies, noted Va, are introduced as mixing constituents. Early examples of this case can be found in the study of the Fe-C system by Gustafson[96] or of Mo-C by Andersson.[97] A general model for such phases is $(A)_a(C,Va)_b$.

In the study of Fe-C,[96] the values a=1 and b=1 have been used for the fcc phase and a=1 and b=3 for the bcc phase. These values are based on the number of octahedral sites per atom of the host structures that can be occupied by carbon. During the study of the system Mo-C,[97] it was noticed that the almost complete filling of the octahedral sites of the fcc lattice corresponds to the carbide MoC_{1-x}, which is stable in this system. Complete filling of the interstitial octahedral sites results in the NaCl protype structure (Strukturbericht B1). Application of the same model for this carbide and the interstitial fcc solution, metastable in this system, allowed using the Mo fcc lattice stability previously determined for the endmember Mo:Va. In the Fe-Mo-C system,[98] a single model was thus used to model both the austenite rich in Fe with a low fraction of C on the interstitial sublattice (y_C) and the carbide with y_C close to one.

In the Mo-C system, three other carbides are stable. They are all based on a hexagonal cell. It was decided[97] that only Mo_2C would be described with the same model as the hcp interstitial solution and that only half of the octahedral interstitial position would be taken into account, i.e., a=1 and b=0.5. This choice is expected to provide a poor estimate of the ideal mixing for materials having an hcp matrix but it has been retained in most of the descriptions of such phases with a few exceptions, such as in the study of Zr-O by Liang et al.[99]

When considering the model $(A)_a(C,Va)_b$, Eq 11 that expresses the molar compositions as function of the sublattice fractions becomes the following:

$$x_A = \frac{a}{a + b(1 - y_{\mathrm{Va}})} \qquad x_C = \frac{b\, y_{\mathrm{C}}}{a + b(1 - y_{\mathrm{Va}})} \qquad \text{(Eq 39)}$$

and the different terms in Eq 12 are then given by

$$^{\mathrm{srf}}G_M = y_{\mathrm{C}} \, {}^{\circ}G_{\mathrm{A:C}} + y_{\mathrm{Va}} \, {}^{\circ}G_{\mathrm{A:Va}} \qquad \text{(Eq 40)}$$

$$^{\mathrm{cfg}}S_M = -\, b R \sum_i y_i \ln y_i \qquad \text{(Eq 41)}$$

$$^{\mathrm{E}}G_M = \sum_v y_{\mathrm{C}} \, y_{\mathrm{Va}} \, (y_{\mathrm{C}} - y_{\mathrm{Va}})^v \, {}^{v}L_{\mathrm{A:C,Va}} \qquad \text{(Eq 42)}$$

The above equations have the quantities per mole of formula unit and they must be divided by $a + b(1 - y_{\mathrm{Va}})$ to obtain molar values.

In Eq 40, ${}^{\circ}G_{\mathrm{A:C}}$ is the Gibbs energy of the compound where the second sublattice is fully occupied by C and ${}^{\circ}G_{\mathrm{A:Va}}$ is the Gibbs energy of the pure element A. The expression used to evaluate this kind of function has been discussed in sections 2.1 and 2.3.2.

Two different crystal structures, such as A1 and B1, although related, are thus described with this model. In binary systems, usually either the pure element or the compound is stable with a few exceptions, such as the Pu-C system[100] where neither phase has any significant solubility. However, in in some ternary systems, such as C-Mo-Re,[101] an extended solution exists between the two phases, justifying this modeling.

2.5.4 Intermetallic Phases

Intermetallic phases appear in many metallic materials. Their presence can be desired or detrimental. The modeling of their stability ranges is one of the challenges that the Compound Energy Formalism has to face. In this section, we will consider three quite different cases. The first case will be the example of the modeling the non-stoichiometry of the σ phase without any degree of freedom in its constitution. The second case will be the C15 Laves phase modeled with substitutional defects and finally phases showing order–disorder transitions will be discussed. This section ends with a discussion of the use of FP results to assess the Gibbs energy of the endmembers to properly describe such phases.

a. The σ Phase

The σ phase is one of the first intermetallic phases that was modeled using the sublattice model. It is important to properly describe this phase because it is a detrimental phase occurring in steels. The structure of this phase (Prototype CrFe, Pearson symbol tP30, Space group $P4_2/mnm$, Strukturbericht $D8_b$) has 5 different Wyckoff positions. It is stable in many binary systems with very different topologies of homogeneity ranges. In the first descriptions, a general model $(B)_a(A)_b(A,B)_c$ was used. In a binary system, such a model allows description of the phase between two endmembers $B_{a+c}A_b$ and B_aA_{b+c}. As for the cases discussed so far, there is no degree of freedom between the composition of the phase and the sublattice site fractions. Equation 11 can be simply written as follows:

$$x_A = \frac{b + c\,y_A}{a+b+c} \quad \text{and} \quad x_B = \frac{a + c\,y_B}{a+b+c} \qquad \text{(Eq 43)}$$

The concept of "large" A atoms occupying sites with large coordination numbers, "small" B atoms occupying sites with smaller coordination numbers and a mixture of both types of elements on sites with intermediate coordination numbers was introduced. The values of a, b, and c were initially taken as 10, 4 and 16, respectively.[58] They were obtained by merging Wyckoff sites with similar coordination numbers.

However, such a model was not able to treat all the compositions observed experimentally. The model was consequently modified using the values 8, 4 and 18 for a, b and c[102] for convenience. The model had lost part of its connection to the crystal structure but the simplicity of the model was maintained. Later, it was recommended to return to the ratio 10/4/16, allowing mixing of the different elements in two of the sublattices.[103]

To describe the Gibbs energy of the endmembers, a linear function of temperature was added to a weighted sum of the Gibbs energies of the elements in their paramagnetic fcc and bcc states. The assumption made was that the contribution for an element is similar to that of the fcc state when it occupies a sublattice with a small coordination number and similar to that of the bcc state when occupying a sublattice with a large coordination number[102]

$$^{\circ}G^{\sigma}_{A:B:C} = a\ ^{\circ}G^{fcc}_{A} + b\ ^{\circ}G^{bcc}_{B} + c\ ^{\circ}G^{bcc}_{C} + \alpha + \beta\ T \qquad \text{(Eq 44)}$$

For some endmembers the values of α and β were assessed in order to fit the experimental information of the system under consideration. In many of the systems under consideration, such as Cr-Fe[102] or Fe-Mo,[92] the β variable was negative in order to stabilize the phase at higher temperature and to make sure that it does not appear at lower temperatures. However, when dealing with multicomponent databases having many endmembers, these variables were set equal to zero due to a lack of experimental information, as was the case for the compounds in the Cr-Fe-Ni system assessed by Hillert and Qiu.[104]

Hertzman and Sundman[58] used no excess parameters in their initial description of this phase. However, it soon became clear that these had to be used in particular when considering ternary systems, such as in the study of the Fe-Cr-Mo system by Andersson and Lange.[92]

With the improvements in computational power and the possibility of using FP results, more complex models have been introduced for this phase, as will be discussed in section 2.5.4.d and further in sections 3.3.2 and 3.4.

b. The C15 Laves Phase

The different cases discussed so far have in common that there is a unique occupation of the sublattice able to describe one composition of the phase. We will now consider cases where a degree of freedom is allowed in the constitution of the phases. For a given composition, the site occupancy will be defined by a minimum of the Gibbs energy for a given composition of the phase. An example of such a phase often modeled with the CEF is the C15 Laves phase.

This phase (Prototype $MgCu_2$, Pearson symbol cF24, Space group $Fd\bar{3}m$) has two different crystallographic sites.

These are 8b and 16c Wyckoff positions. In the prototype, they are mostly occupied by Mg and Cu, respectively. The ideal composition for this phase is thus $MgCu_2$. However, the phase shows a small composition range of stability around its ideal composition because the two elements substitute each other. The phase can thus be schematized as $(A,B)_8(A,B)_{16}$ or more simply, taking 1/8 of the unit cell as formula unit, $(A,B)_1(A,B)_2$.

Considering the more general case of a phase modeled $(A,B)_{a_1}(A,B)_{a_2}$, the composition of the element i in the phase is linked to the occupation in the two sublattices by the following equation corresponding to the Eq 11 in the present case.

$$x_i = \frac{a_1\, y_i^{(1)} + a_2\, y_i^{(2)}}{a_1 + a_2} \qquad \text{(Eq 45)}$$

Figure 2(a) represents all possible configurations for a phase modeled $(A,B)_1(A,B)_2$ whose ideal composition is AB_2. The x axis is the fraction of occupation by B of the first sublattice, $y_B^{(1)}$. This sublattice is mostly occupied by A in the ideal compound. When $y_B^{(1)}$ increases from 0 to 1, the fraction of A in this sublattice, $y_A^{(1)}$, decreases accordingly from 1 to 0. The y axis is the fraction of occupation by B of the second sublattice, $y_B^{(2)}$. This fraction is equal to 1 in the ideal compound. When $y_B^{(2)}$ increases from 0 to 1, the fraction of A in this sublattice, $y_A^{(2)}$, decreases from 1 to 0. The corner (0,0) thus represent the compound without B, i.e., the compound where both sublattices are occupied by A. This is an hypothetical state that is not accessible experimentally. From pure A in the C15 structure, when increasing $y_B^{(2)}$ to 1, the ideal compound is obtained when the first sublattice is fully occupied by A and the second by B. Starting again from the corner (0,0), increasing $y_B^{(1)}$ to 1 yields a metastable compound where each sublattice is occupied by the "wrong" element with respect to the ideal compound, i.e., it is full with defects. It corresponds to the composition BA_2. In the Cu-Mg binary system, a compound $CuMg_2$ is stable but it has the C_b Strukturbericht structure. A compound with this composition is not stable in the C15 structure and cannot be studied experimentally.

Experimental information on the C15 phase is only available close to the composition of the ideal compound. The assessment of the Gibbs energy of the other endmembers is more difficult. In the first sublattice model description of this phase, Coughanowr et al.[105] used the equivalence to the Wagner-Schottky formalism to express the Gibbs energy of the endmember full of defects.

$$^{\circ}G_{B:A} = {}^{\circ}G_{A:A} + {}^{\circ}G_{B:B} - {}^{\circ}G_{A:B} \qquad \text{(Eq 46)}$$

They assessed the Gibbs energy of the pure elements in the C15 structure to describe the range of non-stoichiometry of the phase. However, this approach has rapidly shown limitations as the values derived for a pure element in different binary systems were different. A unique value of 5 kJ/mol of atoms independent of the element under consideration was used, for example, in the study of Cr-Nb by Costa Neto et al.[106] The range of stability of the phase was assessed using the interaction parameters.

In a first approximation, four different interaction parameters can be considered in the excess term: $L_{A,B:A}$, $L_{A,B:B}$, $L_{A:A,B}$, $L_{B:A,B}$. Each of them mostly affects the mixing along one side of the square in Fig. 2(a). For instance $L_{A,B:B}$ mostly affects the Gibbs energy along the upper side of the square, i.e., between A:B and B:B. This parameter will thus be used to fit the extension of the compounds for compositions richer in B than the ideal compound. The parameter controlling the extension of the compound towards higher A content is $L_{A:A,B}$. The other two interaction parameters have virtually no influence on the stable configuration of the phase. They have often been set equal to the other two considering that the interaction between the two elements is independent of the occupation of the other sublattice, i.e., $L_{A:A,B} = L_{B:A,B}$ and $L_{A,B:A} = L_{A,B:B}$.

The use of the notation * has been introduced in order to handle these parameters more efficiently in a multicomponent database. $L_{A,B:*}$ thus contributes to the Gibbs energy of the phase with $y_A^{(1)}\, y_B^{(1)}\, L_{A,B:*}$ while $L_{A,B:C}$ contributes with $y_A^{(1)}\, y_B^{(1)}\, y_C^{(2)}\, L_{A,B:C}$. When both terms appear in a database both are used by Thermo-Calc[64] and OpenCalphad.[107] In a ternary system, for a phase modeled (A,B)(C,D,E), the two parameter sets shown in Table 1 are identical for the Thermo-Calc or OpenCalphad software.

As already discussed in section 2.3.3, these interaction parameters can also have a RK dependence on the site occupation of the sublattices. Such composition dependence has to be introduced carefully as there are not always enough experimental data to assess the parameters correctly. High orders of these parameters can induce stabilization of the phase in unexpected composition or

Table 1 Additive feature of excess parameters including "*"

$L_{A,B:*} = \alpha$	$L_{A,B:C} = \alpha + \beta$
$L_{A,B:C} = \beta$	$L_{A,B:D} = \alpha$
	$L_{A,B:E} = \alpha$

In Thermo-Calc or OpenCalphad, the parameters in the two columns correspond to the same contribution in a phase that is modeled as $(A,B)_{a1}(C,D,E)_{a2}$

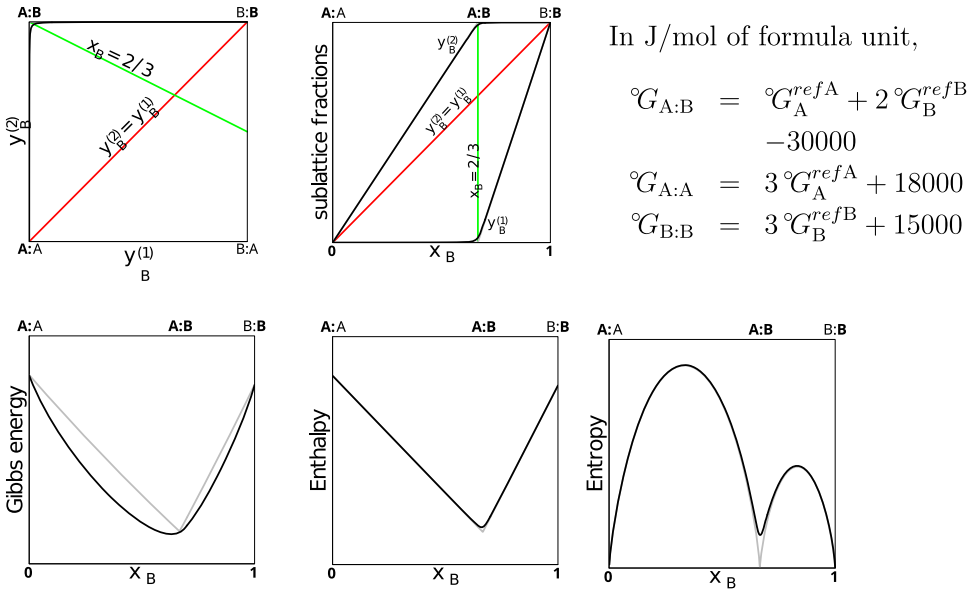

Fig. 2 Results of a schematic model $(A,B)(A,B)_2$ calculated at 1000 K (black lines) and 100 K (gray lines) with the parameters given in 2(c) and Eq 46. 2(a) represents the site fraction of B in the second sublattice versus the site fraction of B in the first sublattice. The green line corresponds to the composition of the ideal compound AB_2. There is a degree of freedom along this line. The actual site fraction is given by the minimization of the Gibbs energy for this composition. The red line corresponds to the disordered state where the occupation is identical in the two sublattices. The black line shows the occupation corresponding to the minimum Gibbs energy for the phase for each composition between pure A and B at 1000 K. 2(b) represents the site fraction of B in the two sublattices versus the composition of the phase. 2(d), 2(e) and 2(f) represent the Gibbs energy, the enthalpy and the entropy of the phase, respectively, versus the composition of the phase

temperature ranges or result in bad extrapolations to higher-order systems.

c. Phases with order–disorder transitions

Ordered phases have the potential to disorder. A phase is disordered when the constituent fractions in all sublattices are the same as the mole fractions. This is represented by the red line in Fig. 2, everywhere else in the constitution square the phase is ordered. Figure 2 is drawn for the case where a_1=1 and a_2=2 but a similar line exists for other values of a_1 and a_2. This allows using a single model for phases displaying an order–disorder relationship. This approach was first applied to Al-Ni by Ansara et al. in 1988[108] where the fcc ordering occurs between the ordered $L1_2$ (a_1=0.75, a_2=0.25) and the disordered A1 phases, and to Fe-Si by Lacaze and Sundman in 1991[109] where the bcc ordering occurs between the ordered B2 (a_1=0.5, a_2=0.5) and the disordered A2 phases. In the latter case, having a single Gibbs energy expression for the two phases is essential as there is a second-order transition between them.

When such phases are described, the endmembers corresponding to pure elements represent the disordered phase. They are often stable, contrary to the case of the intermetallic phases discussed in section 2.5.4.b. In the case of the B2 phase, the two endmembers corresponding to the stoichiometric compounds are actually the same crystallographic state, just shifted by half of the diagonal of the cell. Consequently, they must have the same Gibbs energy. For the $L1_2$ phase, such an equivalence is generally not true, but it is not uncommon for both phases to be stable, as in the Au-Cu system, in contrast to phases showing no disorder.

Description both of the ordered and disordered phases requires the Gibbs energy to display an extremum for any deviation from the disordered state resulting in constraints for the individual model parameters. Such constraints were introduced by Ansara et al. in the case of the Ni_3Al phase[108] and in the simpler B2 case by Lacaze and Sundman.[109] The constraints derived are rather complex and difficult to apply to multicomponent databases. This led to the introduction of a new formalism discussed in section 3.3.1.

d. Inputs from density functional theory

One of the challenges in using the CEF is the need to assess the Gibbs energy of metastable compounds. The use of Density Functional Theory (DFT) allows calculation of the formation energies of these compound to overcome this issue.

When discussing the modeling of the C15 Laves phase in section 2.5.4.b, we explained that the value 5 kJ/mol of atoms, independent of the element, was used for some time. This rough approximation was abandoned when it became possible to obtain values for these metastable endmembers using FP results. Sluiter[110,111] presented a

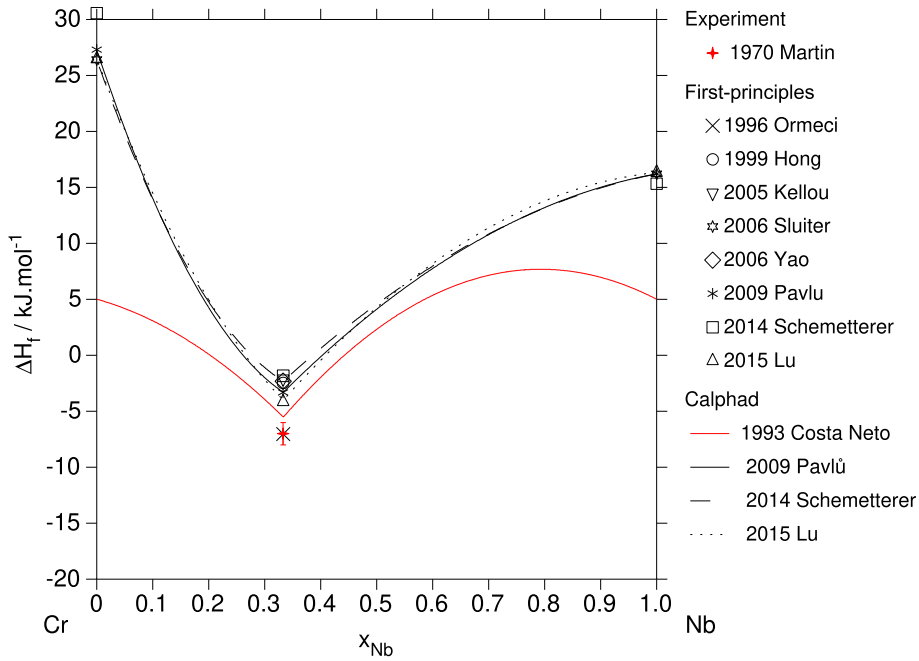

Fig. 3 Impact of changing the lattice stabilities for the pure elements when modeling the C15 phase in the Cr-Nb system

systematic study of different intermetallic structures for the pure elements that formed the basis of a new set of lattice stabilities for intermetallics.

Figure 3 compares the enthalpy of formation of the C15 phase in the Cr-Nb system as described in different Calphad studies to an experimental value[112] and several FP results.[110,113-119] It is interesting to note that the use of FP values for the lattice stabilities of the pure elements in this phase induces different curvature of the curves close to the ideal composition of the phase. While Costa Neto et al.,[106] using the 5 kJ/mol value for both elements, needed repulsive interactions to be able to describe the system, later works using values from DFT[117-119] present a stabilizing interaction when Cr is substituted in the Nb site, i.e., when the small atom enters in the position of the larger one and destabilizing when Nb enters the Cr site. This is physically more satisfactory than the behavior obtained when the 5 kJ value was used.

DFT results can actually be used to estimate not only the Gibbs energy of pure elements in metastable states but of many metastable compounds for which it is not possible to perform experimental studies. For example, it has been shown by Fries and Sundman[120] for the σ phase in the Re-W system and by Dupin et al.[121] for the μ phase in the Nb-Ni system that using DFT results for the compounds with a CEF description considering 5 sublattices, i.e., as many as Wyckoff positions, allows calculation of site occupancies that are very close to those obtained from CVM calculations using the same DFT results.

The use of FP results is thus of great interest for describing many metastable configurations as it allows using models that reflect the crystallographic structure of the phases, avoiding the approximations introduced in the early models to limit the number of endmembers, as discussed in section 2.5.4.a.

For example, while descriptions of the C14 and C36 Laves phases have often been simplified with only 2 sublattices, thanks to the use of DFT results, recent work by Hallstedt[122] takes into account the larger number of Wyckoff positions. However, the best way to use these FP results is still under discussion. For some phases, it appears enough to consider a constant lattice stability. For others that have a Gibbs energy closer to the stable states, it seems important to derive a difference in vibrational entropy between the stable and intermetallic phases for the pure elements, as shown by Matthieu et al.[123] and Pereira dos Santos et al.[124]

2.5.5 Modeling Oxides and Other Ionic Solids

Some phases are sufficiently ionic that their possible composition range is dictated by the charge of the constituents occupying the crystallographic sites (sublattices). Such phases can only be reasonably modeled when ions are used within the CEF. The CEF can then be directly formulated from the crystal structure and defect chemistry of the respective phase. So far, a major part of CEF modeling with ions has concerned oxides, but sulfides are also similarly ionic and halides are even more ionic. Nitrogen falls somewhat in between; in alloys, including nitrides, it is usually treated as neutral, whereas in SiAlON ceramics it has been treated as ionic.[125] The CeO_{2-x} fluorite phase

was the first phase with ions to be modeled using the CEF by Hillert and Jansson,[126] although at that time it was described as a special case of the two-sublattice Hillert-Staffansson model. Shortly thereafter a more general description of the use of ions within the CEF was published by Hillert et al.[127] Therein, examples were given for several complex oxides; magnetite (Fe_3O_4), orthopyroxene ($(Fe,Mg)SiO_3$) and olivine ($(Fe,Mg)_2SiO_4$). Barry et al.[128] and Degterov et al.[129] give examples for the use of the CEF for phases with ions.

The energy cost for any deviation from electric neutrality on a macroscopic scale is forbiddingly high, so that any phase can be considered to be electrically neutral. Thus, an electroneutrality condition is applied to the CEF, i.e., only neutral compositions are allowed to take part in any equilibrium calculation. The neutrality condition reduces the dimensionality of the CEF model by one. Since the CEF endmembers can be charged, this means that one charged endmember must be given an arbitrary value (called a charged reference). This value can only be defined once for each phase. When the same phase has been modeled in different systems using different charged references the models can only be combined when the charged reference for one instance of the phase is changed to be the same as for the other instance. Also, not all neutral compounds directly correspond to a single endmember. Such neutral compounds will then have to be expressed as a sum of endmembers, which will also include an expression for the ideal entropy of mixing.

Many oxides are stable in the simple NaCl (halite, B1) structure. One of them is FeO (wüstite) which shows an unusually wide composition range. It is not even stable at the stoichiometric composition FeO so that it is more appropriately written $Fe_{1-x}O$. The normal oxidation state of Fe in FeO is +2, but it can easily be oxidized to +3. To compensate for the higher charge, vacant sites are formed on the cation sublattice; one vacancy for every two Fe oxidized from +2 to +3. In principle, the higher Fe oxidation state could also be compensated by forming interstitial oxygen ions, but the energy cost for this is much higher. The oxidation of Fe can be written as

$$2Fe_{Fe}^{\times} + \frac{1}{2}\ O_2(g) \rightarrow 2Fe_{Fe}^{\bullet} + Va''_{Fe} + O_O^{\times} \qquad \text{(Eq 47)}$$

in Kröger-Vink notation. Here, $Fe_{Fe}^{\times}$ means an Fe on an Fe lattice site with nominal charge (i.e., Fe^{+2}), $Fe_{Fe}^{\bullet}$ is an Fe on an Fe lattice site with one positive charge relative to the nominal charge (i.e., Fe^{+3}) and Va''_{Fe} is a vacant Fe site with two negative charges relative to the nominal charge (i.e., a neutral vacancy). The corresponding CEF model is

$$(Fe^{+2}, Fe^{+3}, Va)_1(O^{-2})_1. \qquad \text{(Eq 48)}$$

This model generates the endmembers Fe^{+2}:O^{-2}, Fe^{+3}:O^{-2} and Va:O^{-2}. The first endmember is neutral, corresponding to stoichiometric FeO, and the following two have the charge +1 and −2. The latter two can be combined to form the neutral compound $Fe_{2/3}O$, more conveniently written $FeO_{1.5}$ or Fe_2O_3 (not to be confused with the stable phase Fe_2O_3, which has the corundum crystal structure). The Gibbs energy of this (neutral) compound can be written as

$$G_{Fe_{2/3}O} = \frac{1}{3}\left(2\,{}^{\circ}G_{Fe^{+3}:O^{-2}} + {}^{\circ}G_{Va:O^{-2}} + 3\ RT\left(\frac{2}{3}\ln\frac{2}{3} + \frac{1}{3}\ln\frac{1}{3}\right)\right). \qquad \text{(Eq 49)}$$

This CEF model can be visualized in a triangular diagram shown in Fig. 4. Only compositions on the neutral line connecting FeO and $Fe_{2/3}O$ are possible. The endmember Va:O^{-2} is shared by other cations when the model is extended to higher order systems and was, therefore used as the charged reference and given the value zero by Sundman[82] when modeling the Fe-O system (${}^{\circ}G_{Va:O^{-2}} = 0$). To somewhat simplify the modeling when more complex CEF models are used, the charged reference can be given a value corresponding to its stoichiometry, which in this case would be ${}^{\circ}G_{Va:O^{-2}} = \frac{1}{2}\ {}^{\circ}G_{O_2}$. This kind of charged reference was, e.g., used for several phases in the La_2O_3-SrO system.[130] However, the former value is commonly accepted when modeling the B1-oxide phase and changing the charged reference is not completely trivial. To describe the actual experimental data on the $Fe_{1-x}O$ phase, further interactions are needed. There are three possible pair interactions, corresponding to the three sides of the triangle in Fig. 4. The $Fe^{+3}-Va$ interaction has no influence along the neutral line and the $Fe^{+2}-Va$

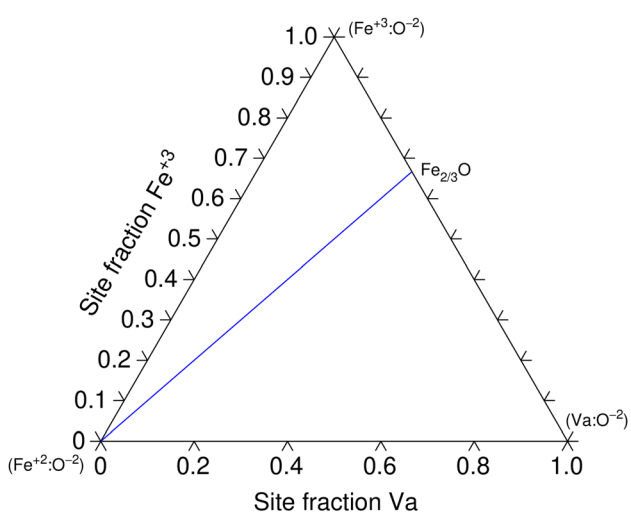

Fig. 4 The CEF model for $Fe_{1-x}O$. The corners represent the CEF endmembers, two of which are charged, and the line connecting the neutral compounds FeO and $Fe_{2/3}O$ shows possible neutral compositions

interaction is shared with other systems, so that only the $Fe^{+2}-Fe^{+3}$ interaction remains to be fitted to experimental data.

In general, the number of neutral compounds (i.e., neutral combinations of endmembers) that can be described using experimental data is less (often much less) than the number of endmembers. Even after the charged reference has been determined there are often several undetermined endmembers. They can be related to the already determined endmembers using reciprocal relations. Typically, the Gibbs energies of these reciprocal relations are set to zero, but they can also be used as an alternative to normal interaction parameters since they have a similar influence for neutral compositions. Failure to control the Gibbs energies of the reciprocal relations can result in a strange behavior of the phase.

The perovskite ($CaTiO_3$) crystal structure is very common among oxides. The perovskite structure can be viewed as an fcc structure with the oxygen ions located at the faces, the larger cation (Ca in this case) at the corners and the smaller cation (Ti) at the central octahedral interstitial site. The ideal perovskite structure is cubic, but many perovskites are non-cubic. This will not be discussed further here as this does not influence the CEF modeling. Here we will use $LaMnO_3$ as an example. $LaMnO_3$ is used as a cathode material in solid oxide fuel cells (SOFC), usually doped with Sr.[131] $LaMnO_3$ shows non-stoichiometry both with respect to the La/Mn ratio (in both directions) and the oxygen content. This is a result of Mn being present in the oxidation states +2, +3 and +4, which also leads to a high electrical conductivity. The resulting defect chemistry is fairly complex, but can be expressed in a CEF model. A detailed description of the modeling of the $LaMnO_3$ perovskite is given by Grundy et al.,[132] including Sr[133] and a comparison with a classic defect chemistry treatment.[134]

Under reducing conditions Mn^{+3} is reduced to Mn^{+2} and vacancies are formed on the oxygen sublattice. This can be expressed by the defect chemical reaction

$$2\ Mn_{Mn}^{\times} + O_O^{\times} \rightarrow 2\ Mn'_{Mn} + Va_O^{\bullet\bullet} + \frac{1}{2}\ O_2(g) \qquad \text{(Eq 50)}$$

which is represented by the CEF model

$$(La^{+3})_1(Mn^{+2}, Mn^{+3})_1(O^{-2}, Va)_3. \qquad \text{(Eq 51)}$$

In addition to the neutral endmember $LaMn^{+3}O_3$ it generates the neutral compound $LaMn^{+2}O_{2.5}$ whose Gibbs energy can be written as

$$G_{LaMn^{+2}O_{2.5}} = \frac{5}{6}{}^{\circ}G_{La:Mn^{+2}:O} + \frac{1}{6}{}^{\circ}G_{La:Mn^{+2}:Va} + 3\ RT\left(\frac{5}{6}\ln\frac{5}{6} + \frac{1}{6}\ln\frac{1}{6}\right) \qquad \text{(Eq 52)}$$

where charges have been left out when there is no ambiguity. Two endmembers are required for this Gibbs energy expression. Under oxidizing conditions Mn^{+3} is oxidized to Mn^{+4}. To compensate for this, an equal amount of vacancies is formed on each cation sublattice in order to keep the La/Mn ratio constant. The defect chemical expression for this can be written as

$$6\ Mn_{Mn}^{\times} + \frac{3}{2}\ O_2(g) \rightarrow Va_{La}''' + Va_{Mn}''' + 6\ Mn_{Mn}^{\bullet} + 3\ O_O^{\times}. \qquad \text{(Eq 53)}$$

i.e., there is a cation deficiency rather than an oxygen excess. This is represented by the CEF model

$$(La^{+3}, Va)_1(Mn^{+3}, Mn^{+4}, Va)_1(O^{-2})_3. \qquad \text{(Eq 54)}$$

This model generates the two neutral compounds $La_{2/3}Mn^{+4}O_3$ and $LaMn_{3/4}^{+4}O_3$. The first is La deficient and the second is Mn deficient. Their Gibbs energies can be written as

$$G_{La_{2/3}Mn^{+4}O_3} = \frac{2}{3}{}^{\circ}G_{La:Mn^{+4}:O} + \frac{1}{3}{}^{\circ}G_{Va:Mn^{+4}:O} + RT\left(\frac{2}{3}\ln\frac{2}{3} + \frac{1}{3}\ln\frac{1}{3}\right) \qquad \text{(Eq 55)}$$

and

$$G_{La:Mn_{3/4}^{+4}O_3} = \frac{3}{4}{}^{\circ}G_{La:Mn^{+4}:O} + \frac{1}{4}{}^{\circ}G_{La:Va:O} + RT\left(\frac{3}{4}\ln\frac{3}{4} + \frac{1}{4}\ln\frac{1}{4}\right). \qquad \text{(Eq 56)}$$

The complete CEF model is then

$$(La^{+3}, Va)_1(Mn^{+2}, Mn^{+3}, Mn^{+4}, Va)_1(O^{-2}, Va)_3. \qquad \text{(Eq 57)}$$

This model generates 15 endmembers, which can be expressed in terms of the four neutral compounds defined above. The last (16th) neutral endmember corresponds to the empty crystal when all three sublattices are filled with vacancies. It would be tempting to set $G_{Va:Va:Va}$ to zero, but this does not work. This Gibbs energy represents the formation of defects on all three sublattices simultaneously and in Ref 132 a Wagner-Schottky type expression was

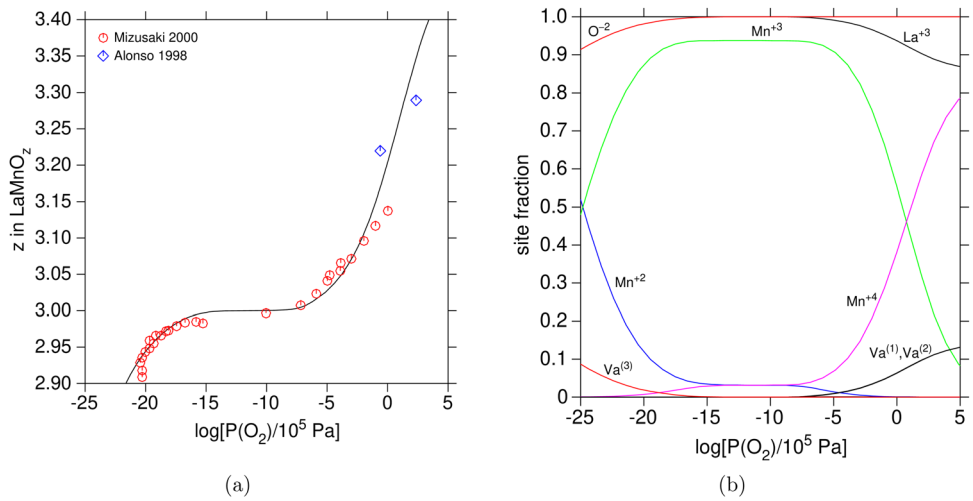

Fig. 5 In (a) the oxygen content in $LaMnO_3$ as function of oxygen partial pressure at 1073 K using the CEF model from Grundy et al.[132] with experimental data from Mizusaki et al.[135] and Alonso.[136] Further experimental data points are included in the original assessment. In (b) the site fractions in $LaMnO_3$ at 1073 K along the curve in (a)

used to define its energy. This worked well for $LaMnO_3$, but it is unclear how to handle this for other perovskites since this value can only be set once for all perovskites. It would not make sense having the Gibbs energy for $LaMnO_3$ appearing in the model, e.g., $CaTiO_3$. After defining a charged reference, the remaining endmembers can be related by 10 reciprocal reactions whose Gibbs energies are all set to zero. The Gibbs energies of all endmembers can thus be unequivocally determined. The set of neutral compounds determined above considering possible defects is not unique. Further neutral compounds can be defined, but those are redundant. In the full model defined by Grundy et al.[132] antisite Mn^{+3} is also included on the first sublattice, but this is of relatively minor importance. The oxygen content in $LaMnO_3$ as function of oxygen partial pressure using this CEF model is shown in Fig. 5(a) at 1073 K. The site fractions in $LaMnO_3$ at the same conditions are shown in Fig. 5(b). It is interesting to note that the site fraction of Mn^{+3} only reaches a maximum of about 0.94 (not unity), i.e., even at perfect stoichiometry Mn^{+3} is noticeably dissociated into Mn^{+2} and Mn^{+4}.

Detailed accounts of the modeling of the fluorite phases CeO_2[126,137] and UO_2[100,138] and the spinel phases Fe_3O_4[82] and $MgAl_2O_4$[139] are given elsewhere. The same concepts were used to model the defect chemistry in the semi-conductor phases GaAs by Hillert and Chen[140] and CdTe by Chen et al.[141]

3 Evolution of the Original Formalism

The initial formalism gave birth to different kinds of evolution. We will first consider the implementation meant to model strong order of ionic liquids. We will then explain how CEF can approximate SRO in crystalline phases. In section 3.3, two formalisms splitting the Gibbs energy into several sets of composition variables will be discussed. The recent EBEF where the endmember energies are replaced by bond energy parameters between pairs, triangles and higher order configurations but keeping the ideal configurational entropy on the sublattices will then be presented. Finally perspectives of improved models for oxides will be discussed.

3.1 Back to the Liquid

The sublattice model can describe Long Range Order (LRO) but not Short Range Order (SRO), i.e., when atoms in a condensed phase may locally prefer a different arrangement of atoms on adjacent sites than the global arrangement on the sublattices.

For the liquid phase the Temkin model[25] is an LRO model but in principle there is only SRO as there are no lattice sites. However, strong electrostatic forces makes it reasonable that cations and anions can be distributed randomly only on sites which are already occupied by the same type of ion, as with the Temkin model.

A model for SRO in the liquid is the associate model[142-144] in which molecular-like aggregates with a composition close to the maximum SRO are assumed to mix randomly with the atoms. This can reasonably describe weak SRO and can work well in a binary system but creates problems in higher order systems when several SRO associates are present and their interaction is difficult to estimate. Instead, a new extension of the Temkin model was developed, called the partially Ionic 2 Sublattice Liquid, (I2SL), and is described below.

Pelton et al.[145] developed a modified quasichemical model for liquids and later incorporated the Temkin model which was named Modified Quasichemical Model in the Quadruplet Approximation (MQMQA).[146] It is not implemented in the software used for this paper but it can be used to describe multicomponent liquids of many different types with similar results as those obtained using the I2SL model.

The partially ionic 2-sublattice liquid (I2SL) model is not a CEF model because the site ratios are not constant. The development of this model by Hillert et al.[147] is based on the experience gained from an assessment of the Fe-S system by Fernàndez Guillermet et al.,[57] combined with a creative use of the sublattice concepts that involve addition of new features to the Temkin model.

In contrast to the original Temkin model,[25] the number of sites on the cation and anion sublattices in the I2SL model are allowed to vary, in order to maintain electroneutrality. In the anion sublattice a charged vacancy was introduced to handle systems without real anions and also neutral constituents:

$$(\mathrm{C}^{+})_{P}(\mathrm{A}^{-},\mathrm{Va}^{-Q},\mathrm{B})_{Q} \qquad \text{(Eq 58)}$$

where C^{+} are cations, A^{-} are anions, Va^{-Q} is a vacancy with the induced charge $-Q$ (equal to the number of sites on the anion sublattice) and B are neutrals, which can represent compounds such as $\mathrm{FeO}_{1.5}$. The site ratios are the sum of the charges on the opposite sublattice to maintain electroneutrality:

$$P = \sum_{j} -q_j y_j + Q y_{\mathrm{Va}} \qquad \text{(Eq 59)}$$

$$Q = \sum_{i} q_i y_i \qquad \text{(Eq 60)}$$

where q_j is the (negative) charge and y_j the fraction of anion $j \in \mathrm{A}^{-}$ and q_i is the charge and y_i the fraction of cation $i \in \mathrm{C}^{+}$. Note that if there are no anions the charge on the vacancies balances that of the cations and $P = Q$. The neutrals do not affect the site ratios.

The surface of reference and configurational terms in the generic Gibbs energy expression, Eq 12, are:

$$^{\mathrm{srf}}G_M = \sum_{i}\sum_{j} y_i y_j \, {}^{\circ}G_{\mathrm{C}_{q_\mathrm{A}}\mathrm{A}_{q_\mathrm{C}}} + Q y_{\mathrm{Va}} \sum_{i} y_i \, {}^{\circ}G_{\mathrm{C_i:Va}} + Q \sum_{k} y_k \, {}^{\circ}G_{\mathrm{B}_k} \qquad \text{(Eq 61)}$$

$$^{\mathrm{cfg}}S_M = -RP \sum_{i} y_i \ln(y_i) - RQ\left(\sum_{j} y_j \ln(y_j) + y_{\mathrm{Va}} \ln(y_{\mathrm{Va}}) + \sum_{k} y_k \ln(y_k) \right) \qquad \text{(Eq 62)}$$

where ${}^{\circ}G_{\mathrm{C}_{q_\mathrm{A}}\mathrm{A}_{q_\mathrm{C}}}$ is the Gibbs energy of formation of the neutral compound $\mathrm{C}_{q_\mathrm{A}}\mathrm{A}_{q_\mathrm{C}}$, ${}^{\circ}G_{\mathrm{C_i:Va}}$ is the Gibbs energy of one mole of the cation C_i (charge balanced by the Va) and ${}^{\circ}G_{\mathrm{B}_k}$ the Gibbs energy of one mole of neutral B_k. The configurational entropy assumes random mixing of the constituents on each sublattice. The sum over k is for all neutrals.

The fact that the site ratios P and Q vary with composition must be included in the derivatives of the Gibbs energy expression. As already stated, this is not a CEF model but it would never have been derived without the inspiration of the CEF model. For metallic liquids without anions or neutrals it is equivalent to a regular solution model with random mixing, which was the model used previously. The I2SL model has been successfully used to describe several liquid systems with different anions and neutrals. For a detailed explanation of the excess Gibbs energy see the book by Lukas et al.[148] There are also rules on how to handle elements with multiple charges or weak electronegativity, for example C, that must be considered, see for example Ref 75, 100, 149.

As mentioned in Ref 147 it is interesting to note that a binary A-B system modeled as $(\mathrm{A}^{+q_\mathrm{A}})_P(\mathrm{B}^{-q_\mathrm{B}},\mathrm{Va},\mathrm{B})_Q$ with the I2SL model is mathematically identical to an associated model for the liquid $(\mathrm{A}, \mathrm{A}_1\mathrm{B}_{q_\mathrm{B}/q_\mathrm{A}},\mathrm{B})$ using an electrically neutral associate $\mathrm{A}_1\mathrm{B}_{q_\mathrm{B}/q_\mathrm{A}}$. For ternary and higher order system there is no such equivalence.

In the assessment of a liquid using the I2SL model it may be necessary to estimate one or more metastable endmembers. If the Gibbs energies of the endmembers in a reciprocal subsystem, $(\mathrm{A}^{+},\mathrm{B}^{+})_P(\mathrm{C}^{-},\mathrm{D}^{-})_Q$ in the liquid are very different (which may happen when combining independently assessed binary systems) this may create a so called reciprocal miscibility gap, as described in section 2.3.5 at high T in the liquid. Usually there are no experimental data confirming a stable liquid but such miscibility gaps are unlikely at high T. This problem is discussed in Ref 87,150.

3.2 Approximate Treatment of Short Range Order

The thermodynamic properties of crystalline phases depend on SRO. The Cluster Variation Method (CVM) of Kikuchi,[32] first presented in 1951, provided the variational framework to solve the statistics of lattice gases. Some 20 years later, when computers became available for scientific work, van Baal,[34] using a single nearest neighbor bond energy, u_{AB}, calculated the prototype fcc ordering diagram in the tetrahedron approximation of the CVM (CVM-T) shown in Fig. 6(a). This diagram agreed with experimental observations regarding several aspects of the solid state order–disorder phase transitions: the transitions are first-order type and the correct shapes and topology of single and two phase regions in the vicinity of the order–disorder transitions. A particular feature of the phase diagram is that the maxima of the single-phase regions of the ordered phases $\mathrm{L1}_2$ and $\mathrm{L1}_0$ are separated by a single-phase region of the disordered fcc solid solution phase.

The CVM-T used for the phase diagram in Fig. 6(a) has 16 clusters (which can be considered as endmembers in a

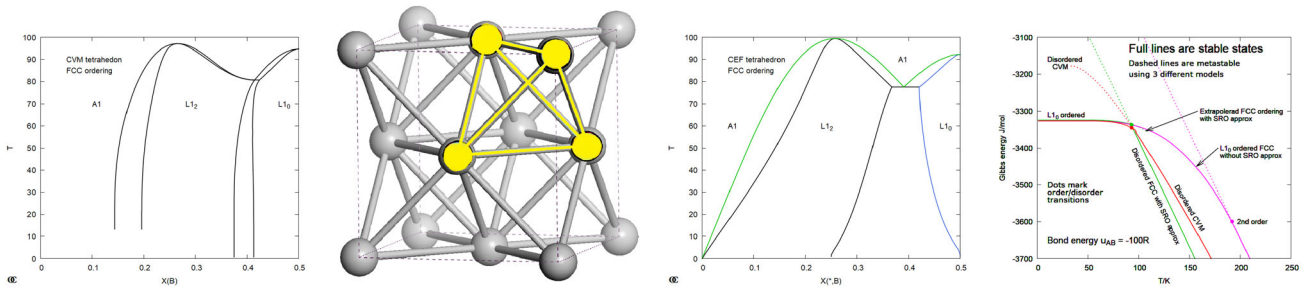

(a) (b) (c) (d)

Fig. 6 In (a) the phase diagram for a prototype fcc ordering using the CVM-T with a nearest neighbor bond energy, $u_{AB} = -100R$. In (b) the tetrahedron cluster used in the CVM-T is marked in yellow. In (c) the calculated phase diagram using a 4 sublattice CEF model together with reciprocal excess parameter equal to the bond energy to approximate SRO. It has a first order transition to disordered fcc at the same temperature as the CVM-T model. In (d) the stable and metastable extrapolations of the Gibbs energy curves for ordered $L1_0$ and disordered states at equiatomic composition using 3 different models, all with the same bond energy. The third model is a 4 sublattice CEF model with no SRO reciprocal parameters as used by Shockley[151] and with this model the $L1_0$ disorders at much higher temperature (Color figure online)

single sublattice): one each for pure A and B, 4 for each combination A_3B and AB_3 and 6 for A_2B_2 on the 4 tetrahedron positions. Assuming a single bond energy, u_{AB}, the Gibbs energy parameters for these endmembers are: ${}^{\circ}G_{A_3B_1} = 3u_{AB}$, ${}^{\circ}G_{A_2B_2} = 4u_{AB}$ and ${}^{\circ}G_{A_1B_3} = 3u_{AB}$. The CVM-T configurational entropy is calculated as:

$$ {}^{cfg}S_M/R = -2\sum_{ijkl} y_{ijkl}\ln(y_{ijkl}) + \sum_{ij}\sum_{st} p_{ij}^{(st)}\ln(p_{ij}^{(st)}) - 5\sum_{i} x_i \ln(x_i), \quad \text{(Eq 63)} $$

where y_{ijkl} are the 16 tetrahedron probabilities, $p_{ij}^{(st)}$ the set of 6 pair probabilities between elements ij on sublattices st and x_i the site probabilites (or mole fractions). This model allows the description of the $L1_2$, $L1_0$ and disordered fcc. The fractions of the 6 different pairs, $p_{ij}^{(st)}$, and the mole fractions, x_i, are summed from the appropriate y_{ijkl} fractions. The equilibrium for the CVM model is obtained by minimizing the Gibbs energy over the 16 endmember fractions subject to the external conditions and internal constraints.

In Fig. 6(d) the Gibbs energy curves at the ideal $L1_0$ composition for various ordering models are plotted as function of temperature. The curves corresponding to the CVM-T just presented are shown in red.

The 4 sublattice fcc model corresponding to the treatment first presented in 1938 by Shockley[151] is shown in magenta. In this model, the four sites constituting the tetrahedron in yellow in 6(b) are treated as distinct sublattices in a CEF model, each occupied by two different elements. The sublattices are equivalent to one another and have the same site fractions in the disordered state. The CEF model has 16 endmembers representing the possible distribution of elements on the sublattices that are similar to the clusters considered by the CVM-T. The configurational entropy is simply the random mixing on the 4 sublattices. There are no contributions from the pair or mole fractions. The same bond energy being used, the ordered state at low temperature has the same Gibbs energy value as the CVM-T but it predicts the order–disorder transition temperature at more than twice the theoretical value.[48]

Finally the green curves correspond to the 4 sublattice CEF where the SRO is approximated by a reciprocal excess parameter explained in section 2.3.5. This model is similar to the one used by Shockley but excess parameters of the type $L_{A,B:A,B:*:*}$ have been added. As indicated by their configuration, they are multiplied by products of site fraction of the type $y_A^{(r)}\, y_B^{(r)}\, y_A^{(s)}\, y_B^{(s)}$. These reciprocal parameters have been shown to be the first order approximation of the CVM configurational entropy by Sundman et al.[152]

Kusoffsky et al.[153] calculated the phase diagram for the prototype fcc ordering shown in Fig. 6(c) using this CEF model together with reciprocal parameters equal to the bond energy, u_{AB}. This approximately accounts for the SRO contribution from the CVM-T model getting much closer to the CVM-T phase diagram and its associated enthalpy and entropy data. In Fig. 6(d), the entropy in the disordered state is ideal according to CEF and slightly overestimated with respect to the CVM-T model. The shift in energy allowing the shift in ordering temperature is thus related to the enthalpy change introduced by the reciprocal parameters that account for the contribution of the clusters not considered by the model. The assessment of the Au-Cu system[152] using reciprocal parameters could reproduce the experimental phase diagram and thermodynamic data, confirming the abiblity of this model to describe real alloys.

This is a very important improvement of the original use of the sublattice model because, as explained in the introduction, the advantage of using CEF is that the equilibrium

calculations are simplified. In a binary system, the CEF model has only 3 independent fraction variables whereas the CVM-T model has 15. This difference increases exponentially with the number of components and the size of the clusters. However, even with reciprocal parameters, the sublattice model for order–disorder transitions cannot describe the rapid increase of the heat capacity close to the order–disorder transition unless a complex temperature dependence is used for the model parameters.

The application of the sublattice model to phases with order–disorder has been discussed in several papers[49,154-160] and it is used in commercial databases like the TCNI for superalloys[161,162] and the TCHEA for high entropy alloys.[163,164] However, these databases do not use a model with 4 sublattices (4SL) as explained in this section but an equivalent of the 2 sublattice (2SL) model.[161,165] Moreover they make use of the formalism presented in section 3.3.2.

These features induce the need to introduce many relationships between the parameters used in order to ensure that the disordered phases are really disordered making the constitution and the handling of a multicomponent database highly demanding. A recent modification of the sublattice model for ordered intermetallics could solve this problem (see section 3.4).

3.3 Splitting the Formalism Using Several Variables

In the Gibbs energy expression in Eq 12 the term ${}^{\mathrm{srf}}G_M$ defines a surface of reference for the modeling of the interactions of the constituents of the phase related to the Gibbs energy of its endmembers. When using models with many sublattices the surface of reference becomes quite complicated and it may be simpler to use, as surface of reference, a model with just one or two sublattices. The available implementations of the application of this idea will be presented in the following.

3.3.1 The 3 Term Formalism

Even though early CEF descriptions of order–disorder transformations[108] were quite satisfactory, the relationships that needed to be introduced between the parameters were too complicated for multicomponent databases. Thus a new formalism was introduced by Ansara et al.[166] that splits the Gibbs energy of the phase into 3 terms using different constitution variables:

$$G_M = G(x_i) + \Delta G(y_i^s) - \Delta G(y_i^s = x_i) \quad \text{(Eq 64)}$$

$$G(x_i) = \sum_i x_i\, {}^{\circ}G_i + RT \sum_i x_i \ln x_i + {}^{\mathrm{phy}}G(x_i) + {}^{\mathrm{E}}G(x_i) \quad \text{(Eq 65)}$$

$$\Delta G(y_i^s) = \sum_I P_I(Y)\, \Delta^{\circ}G_I + RT \sum_s a^s \sum_i y_i^s \ln y_i^s + {}^{\mathrm{phy}}G(y_i^s) + {}^{\mathrm{E}}G(y_i^s) \quad \text{(Eq 66)}$$

The first term in this formalism, $G(x_i)$, corresponds to the Gibbs energy of the disordered phase. Its description can be assessed independently of the ordering contribution but it will affect the equilibria of the ordered phase. In a multicomponent system, it allows to take into account the description of a subsystem previously assessed without considering possible ordering. It allows to treat the magnetic contribution independent of the chemical ordering. The equations above only consider substitutional species and not any interstitial sublattices. Therefore, the expression of $G(x_i)$ corresponds to that of a substitutional solution.[148] It can be more generally based on the CEF, in particular, to describe interstitial solution in a site that is not occupied by the elements undergoing ordering.

The second term, $\Delta G(y_i^s)$, is expressed by Eq 66. It is a function of the site fractions and thus order dependent. It is very similar to the CEF expressed by Eq 12. They differ in the introduction of the symbol Δ in order to emphasize that $\Delta^{\circ}G_I$ has a different reference state than ${}^{\circ}G_I$. $\Delta^{\circ}G_I = 0$ when I is a pure element.

The third term, $\Delta G(y_i^s = x_i)$, also expressed by Eq 66, replaces the site fraction by the molar composition of the phase. The second and third terms thus cancel when the phase is disordered.

As $G(x_i)$ corresponds to the Gibbs energy of the phase when it is disordered, the rest of the expression, $\Delta G(y_i^s) - \Delta G(y_i^s = x_i)$ corresponds to the ordering energy. The formalism does not impose any peculiar meaning to the two parts of this ordering contribution. As discussed by Ansara et al.:[167]

- $\Delta G(y_i^s = x_i)$ could be set zero, making $\Delta G(y_i^s)$ the ordering energy
- or it could be forced to be identical to the formation of the disordered phase from the pure elements in the phase under consideration, $\Delta G(y_i^s = x_i) = G(x_i) - \sum_i x_i\, {}^{\circ}G_i$, making possible to assess the formation Gibbs energy of the endmembers, $\Delta^{\circ}G_I$, from DFT. The excess parameters of $G(x_i)$ can then be expressed as functions of the parameters of $\Delta G(y_i^s)$. Such relations have been derived by Kussofsky et al.[153] in the case of the modeling of the fcc ordering with 4SL.

If $\Delta G(y_i^s = x_i) = G(x_i) - \sum_i G_i$ is not fixed, the use of DFT results is not as straightforward. Even if this formalism has often been used and is the basis of the TCNI database,[161,162] it is difficult to handle due to the freedom

in the meaning of the ordered parameters allowed by the combination of three terms.

Another difficulty in the use of this formalism comes from the fact that the parameters of the CEF in Eq 66 should be linked by constraints in order to ensure the possibility of disorder. Even if this model is often referred to as order–disorder formalism, when such constraints are not properly set, the minimum Gibbs energy of the phase will not occur for the disordered state. When modeling the B2 ordering, these constraints are quite simple; they are based on the fact that the two sublattices are crystallographically equivalent.

When using a 2SL model with the stoichiometry 3/1, such as for the $L1_2$ phase, the constraints are not as obvious; they can be derived solving the equations with the derivatives of the Gibbs energy being equal to zero when the phase is disordered, as introduced by Ansara et al.[108] for a binary case and derived by Dupin[165] for higher order systems. They can also be obtained solving the mathematical equivalence of the 2SL model with a symmetrical 4SL model based on the equivalence of the four sites defining the regular tetrahedra constituting the fcc lattice.[161,165] The equivalence of the crystallography when exchanging atoms implies the equality of the Gibbs energy of the configurations. For instance

$$^{\circ}G_{\mathrm{A:A:A:B}} = {}^{\circ}G_{\mathrm{A:A:B:A}} = {}^{\circ}G_{\mathrm{A:B:A:A}} = {}^{\circ}G_{\mathrm{B:A:A:A}} \quad \text{(Eq 67)}$$

$$^{\circ}G_{\mathrm{A:A:B:B}} = {}^{\circ}G_{\mathrm{A:B:A:B}} = {}^{\circ}G_{\mathrm{B:A:A:B}} = {}^{\circ}G_{\mathrm{A:B:B:A}} = {}^{\circ}G_{\mathrm{B:A:B:A}} = {}^{\circ}G_{\mathrm{B:B:A:A}} \quad \text{(Eq 68)}$$

These relationships have been used for the calculations using the 4SL CEF presented in section 3.2, discussing SRO for fcc solutions.

The use of 4SL allows the description of more phases than 2SL. For the fcc lattice, it allows description of the disordered phase, A1, and also the ordered phases $L1_2$ and $L1_0$.[152,153,165] When considering the bcc phase, 4SL allows descriptions of the A2 as well as the ordered B2, B32 and $D0_3$ or $L2_1$ phases.[168,169] The description of these latter phases with a single equation is of great interest as these phases often show second order transformations between them, as in the system Al-Fe-Ti at 1273 K,[170] and demonstrated in a thermodynamic assessment of this system.[171] The tetrahedron of the bcc lattice is not an ideal terahedron as it has two different bond lengths between the first and second nearest neighbors and the equivalence of the configurations differs from the fcc case where the terahedron is ideal. If the first and third SL are first neighbours then AABB will correspond to a B2 structure while ABAB will be B32

$$^{\circ}G_{\mathrm{A:A:A:B}} = {}^{\circ}G_{\mathrm{A:A:B:A}} = {}^{\circ}G_{\mathrm{A:B:A:A}} = {}^{\circ}G_{\mathrm{B:A:A:A}} \quad \text{(Eq 69)}$$

$$^{\circ}G_{\mathrm{A:A:B:B}} = {}^{\circ}G_{\mathrm{B:B:A:A}} = {}^{\circ}G(B2) \quad \text{(Eq 70)}$$

$$^{\circ}G_{\mathrm{A:B:A:B}} = {}^{\circ}G_{\mathrm{A:B:B:A}} = {}^{\circ}G_{\mathrm{B:A:A:B}} = {}^{\circ}G_{\mathrm{B:A:B:A}} = {}^{\circ}G(B32) \quad \text{(Eq 71)}$$

Some software[64,107] has facilities to set up automatically the permutation of the regular and irregular terahedra like the ones presented here by the Eq 67-71. It also modifies the name of the phases in the outputs based on the order actually calculated for the phase.

Independent of the way the constraints are derived, they must be properly set up not only in the binary systems for which an ordered phase is described, but also in the ternary and quaternary systems based on them.

3.3.2 The 2 Term Formalism

Inspired by the cluster expansion approach,[172] Ansara et al.[173] introduced a new related formalism that they called Extended Calphad Method. It combines the classical CEF with another contribution which is a function of the composition of the phase, i.e., independent of the degree of ordering. The Gibbs energy is thus split into two contributions, one dependent on the composition of the phase and the other on its sublattice occupation:

$$G_M = n_s\, G(x_i) + \Delta G(y_i^s) \quad \text{(Eq 72)}$$

$$G(x_i) = \sum_i x_i\, {}^{\circ}G_i + {}^{\mathrm{phy}}G(x_i) + {}^{\mathrm{E}}G(x_i) \quad \text{(Eq 73)}$$

$$\Delta G(y_i^s) = \sum_I P_I(Y)\ \Delta^{\circ}G_I + RT \sum_s a^s \sum_i y_i^s \ln y_i^s + {}^{\mathrm{phy}}G(y_i^s) + {}^{\mathrm{E}}G(y_i^s) \quad \text{(Eq 74)}$$

The term $G(x_i)$ is called the disordered contribution even if the phase under consideration never disorders. It is also called the configuration independent term. It is expressed for one mole of atoms but it does not represent a phase by itself as it does not have a contribution to the configurational entropy. It simply provides a surface of reference based on the description of the pure elements in this phase. It also allows to model the magnetic contribution in a rather simple way.[124,174] The excess term ${}^{\mathrm{E}}G(x_i)$ is expected to be used to assess the phase stability without modifying the configuration between the different end-members given by $\Delta G(y_i^s)$, in particular when DFT inputs are used to assess the $\Delta^{\circ}G_I$ parameters.

$\Delta G(y_i^s)$ is the ordered contribution or configuration dependent term. Its expression is similar to the one in Eq 12 although Δ symbols are added in order to emphasize that the reference parameters are actually referred to the

functions given in Eq 73. It is expressed for one mole of the modeled formula unit of the phase and it includes the configurational entropy. If no excess parameters are introduced in Eq 73, the parameters $\Delta^{\circ}G_I$ correspond to the ordering Gibbs energy from the pure elements in the structure under consideration. Magnetic and chemical excess interactions dependent of the configuration can also be considered.

This formalism strongly simplifies the handling of databases with many endmembers as the contribution in Eq 73 defines automatically a reference value of all of them while with the classical CEF expressions like the one presented in Eq 44 have to be entered for each of the endmembers.

The separate definition of the reference values makes it is easier to describe phases with a larger number of endmembers, thus allowing descriptions closer to the crystallography of complex phases and accounting for the mixing of many elements in many Wyckoff positions and a better configurational contribution. The σ phase, a simpler model for which has been discussed in section 2.5.4.a is an example of a phase for which a proper estimate of its configuration is important as it varies significantly from one system to another. The use of this formalism has been reported by Hallstedt et al.[168] for the Co-Cr-Re system and by Bratberg et al.[162] for the σ and μ phases in the TCNI database.

3.4 The Effective Bond Energy Formalism

Dupin et al.[54] introduced a new formalism showing a better ability to extrapolate than the CEF when considering more than 2 sublattices. It is based on the 2 term CEF (Eq 72) with the contribution depending on the sublattice fractions and, in a first approximation, it is reformulated as follows:

$$\Delta G(y_i^s) = \Delta^{\mathrm{srf}} G(y_i^s) + RT \sum_s a^s \sum_i y_i^s \ln y_i^s + {}^{\mathrm{E}}G(y_i^s) \quad \text{(Eq 75)}$$

$$\Delta^{\mathrm{srf}} G(y_i^s) = \sum_s \sum_{t>s} \sum_i \sum_{j>i} \left(y_i^s\, y_j^t\, E_{ij}^{st} + y_j^s\, y_i^t\, E_{ji}^{st} \right) \quad \text{(Eq 76)}$$

The parameter E_{ij}^{st} corresponds to the effective energy of the bond linking species i on sublattice s and species j on the t sublattice. For a phase modeled with 5 sublattices, if s is the first sublattice and t the second, this term can also be written $\Delta^{\circ}G_{i:j:*:*:*}$.

This notation is similar to the use of "*" for the excess parameters discussed in section 2.5.4.b. It indicates that the parameter is not dependent on the occupation of the sublattice for which "*" appears. This notation has the same additive features as shown in Table 1. Here it means that no contributions other than bond energies are given for the ordered reference term. Using the CEF, it is equivalent to defining the Gibbs energy of formation of each compound A:B:C:D as follows:

$$\Delta^{\circ}G_{\mathrm{A:B:C:D}} = E_{\mathrm{AB}}^{12} + E_{\mathrm{AC}}^{13} + E_{\mathrm{AD}}^{14} + E_{\mathrm{BC}}^{23} + E_{\mathrm{BD}}^{24} + E_{\mathrm{CD}}^{34} \quad \text{(Eq 77)}$$

This formalism does not significantly modify the model. It simply introduces the possibility to use "*" in the parameters of the ordered reference contribution. This can be extended to terms where more than two constituents are used. E_{ijk}^{stu} denotes the extra energy contribution for the triplet defined by i in s, j in t and k in u. In a more general form, the reference term in Eq 75 can thus be expanded as:

$$\begin{aligned}\Delta^{\mathrm{srf}} G(y_i^s) = &\sum_s \sum_{t>s} \sum_i \sum_{j>i} \left(y_i^s\, y_j^t\, E_{ij}^{st} + y_j^s\, y_i^t\, E_{ji}^{st} \right) \\ &+ \sum_s \sum_{t>s} \sum_{u>t} \sum_i \sum_{j>i} \sum_{k>j} \\ &\left(y_i^s\, y_j^t\, y_k^u\, E_{ijk}^{stu} + y_j^s\, y_i^t\, y_k^u\, E_{jik}^{stu} + \cdots \right) \\ &+ \sum_s \sum_{t>s} \sum_{u>t} \sum_{v>u} \sum_i \sum_{j>i} \sum_{k>j} \sum_{l>k} \\ &\left(y_i^s\, y_j^t\, y_k^u\, y_l^v\, E_{ijkl}^{stuv} + \cdots \right)\end{aligned} \quad \text{(Eq 78)}$$

This formalism was used by Dupin et al.[54] for the γ' phase in Al-Cr-Ni to convert a 4SL 3 term CEF to a description with less parameters. The different effective energies were the variables used during the original assessment of this system. They are more meaningful for a potential user of the database. In addition, by using them the definition of many endmember compounds is avoided which results in databases that are easier to maintain. In this case, a parameter with more than 2 elements was also used in Eq 78 for the ordered contribution of this phase. When using such parameters, the EBEF allows all the flexibility of the original CEF.

Using "*" in ordered reference terms is actually possible within the 2 term formalism following Eq 72 but also with the 3 term formalism presented in Eq 64. It is actually this latter formalism that was used by Dupin et al.[54] for the description of the γ' phase in Al-Cr-Ni.

The more striking result shown by Dupin et al.[54] is a clear improvement in the extrapolation of binary DFT data to higher order systems when using many sublattices. It appears that the most promising way is to use its first approximation, i.e., the EBEF, by determining the effective bond energies from the Gibbs energies of formation obtained from DFT[54,124] calculations. This procedure has to be performed in each of the binary systems which

constitute the complex system under consideration. This is only of interest for cases dealing with more than 2SL, otherwise EBEF and CEF are equivalent.

For description with 3 or more SL Eq 77 can be used to construct a correlation matrix between the CEF formation energies and the EBE parameters. The inverted matrix can be used to obtain the values of the EBE. A classical inversion is not always possible and different pseudo-inversion techniques exist that can always be applied, for example, the Moore-Penrose method implemented in the package NumPy of Python[175] has been applied by Ivanova[176] to treat the case of the σ phase in the Mo-Ni-Re system and by Pereira dos Santos et al.[124] in the Co-Cr-Ni-Re system, also for the σ phase.

The fact that the a classical inversion matrix is not always possible is due to the fact that for cases with more than 3 sublattices, the number of the CEF compounds is larger than the number of EBE parameters. When considering the inversion for a 3SL case, the number of parameters is identical in the two formalisms but the matrix is usual singular because an extra relationship applies:

$$\Delta^\circ G_{\mathrm{A:B:B}} + \Delta^\circ G_{\mathrm{B:A:B}} + \Delta^\circ G_{\mathrm{B:B:A}} = \Delta^\circ G_{\mathrm{B:A:A}} + \Delta^\circ G_{\mathrm{A:B:A}} + \Delta^\circ G_{\mathrm{A:A:B}} = \quad \text{(Eq 79)}$$

$$E^{12}_{\mathrm{AB}} + E^{13}_{\mathrm{AB}} + E^{23}_{\mathrm{AB}} + E^{12}_{\mathrm{BA}} + E^{13}_{\mathrm{BA}} + E^{23}_{\mathrm{BA}} \quad \text{(Eq 80)}$$

In the 3SL case, even if the numbers of parameters in the two formalisms is identical in a binary system, a reduction of the number of parameters is obtained in higher order systems as the interactions between 3 elements are ignored.

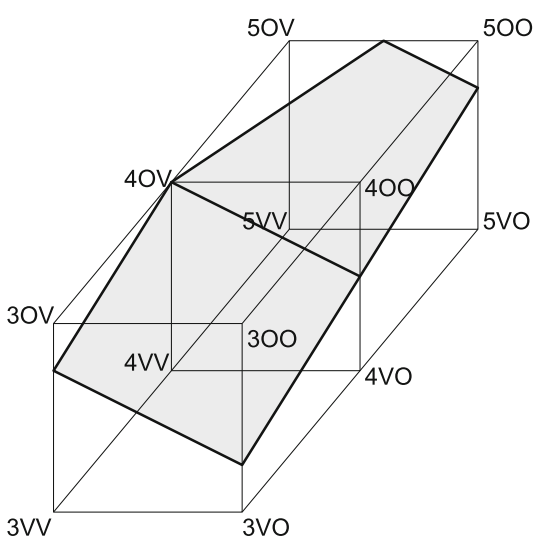

Fig. 7 The CEF model for $UO_{2\pm x}$. The corners represent the CEF endmembers and the grey areas show neutral compositions. The cations U^{+3}, U^{+4}, U^{+5} in the first sublattice and the anions O^{-2} and the vacancies in the second and third sublattices are designated by 3, 4, 5, O, V, respectively

It was shown that the EBEF is better than the CEF[54,124] using only binary DFT information with 5SL for extrapolating the description of the σ phase into multicomponent systems. This is due to the fact that the multicomponent endmembers of the phases considered in these studies can be approximated only from effective bond energies. This could be different for other phases or systems and the interaction between more elements introduced in Eq 78 could then be needed.

3.5 Improved Model for Oxides

Thanks to the introduction of the asterisk, "*", or wildcard explained in section 2.3.5 it is possible to simplify the Gibbs energy parameters for oxide systems where some elements can have multiple charges. Indeed, as several oxidation states are considered to keep the phases electrically neutral, the number of constituents in the sublattices can be large, generating many endmembers whose Gibbs energy must be defined. Moreover, most of them have a net charge and are non-physical.

Using the CEF formalism for oxides, explained in section 2.5.5, the fluorite phase $UO_{2\pm x}$ that exhibits a wide range of hypo- and hyper-stoichiometry of oxygen was modeled by Guéneau et al.[100,177] using the three sublattice model $(U^{+3},U^{+4},U^{+5})(O^{-2},Va)_2(O^{-2},Va)$.

The hypo-stoichiometry, UO_{2-x}, is described by $(U^{+3},U^{+4})(O^{-2},Va)_2(Va)$. Uranium is reduced from U^{+4} to U^{+3} when oxygen vacancies are formed. The hyper-stoichiometry, UO_{2+x}, is modeled by $(U^{+4},U^{+5})(O^{-2})_2(O^{-2},Va)$. Uranium is oxidized into U^{+5} when oxygen interstitials are added on the third sublattice. Twelve endmembers have been described, see Fig. 7.

To model the $UO_{2\pm x}$ phase, it is necessary to assess the Gibbs energies of the following three neutral compounds:

- UO_2, the perfect UO_2 crystal corresponding to the endmember $(U^{+4})(O^{-2})_2(Va)$ with the Gibbs energy:

$$G_{\mathrm{UO_2}} = {}^\circ G_{\mathrm{U^{+4}:O^{-2}:Va}} \quad \text{(Eq 81)}$$

- $UO_{1.5}$ corresponding to the lowest oxygen composition obtained for the site occupation $(U^{+3})(O^{-2}_{0.75},Va_{0.25})_2(Va)$ with the Gibbs energy:

$$G_{\mathrm{UO_{1.5}}} = 0.75\ {}^\circ G_{\mathrm{U^{+3}:O^{-2}:Va}} + 0.25\ {}^\circ G_{\mathrm{U^{+3}:Va:Va}} + 2\ RT(0.75\ln 0.75 + 0.25\ln 0.25) \quad \text{(Eq 82)}$$

with the assessed parameter

$$G_{UO_{1.5}} = G_{UO_2} - 0.5\ G_{1/2O_2(g)} + 338219.1 - 70.22618T$$

- $UO_{2.5}$ which is the highest oxidized composition obtained for the site occupation $(U^{+5})(O^{-2})_2(O^{-2}_{0.5},Va_{0.5})$ with the Gibbs energy:

$$G_{UO_{2.5}} = 0.5\ {}^{\circ}G_{U^{+5}:O^{-2}:Va} + 0.5\ {}^{\circ}G_{U^{+5}:O^{-2}:O^{-2}} + RT\ln 0.5 \quad \text{(Eq 83)}$$

with

$$G_{UO_{2.5}} = G_{UO_2} + 0.5\ G_{1/2O_2(g)} - 58351.62 + 39.67611T$$

While the first neutral compound UO_2 is stable and its properties are experimentally well-established, the other two neutral compounds are outside the stable composition range of the phase. However, their thermodynamic properties can be extrapolated using the experimental oxygen potential data for the phase in its hypo- and hyper-stoichiometric regions.

Simple mass balance equations can then be used to relate the energies of the other endmembers leading to a minimum number of parameters to assess:

$${}^{\circ}G_{U^{+3}:O^{-2}:O^{-2}} - {}^{\circ}G_{U^{+3}:O^{-2}:Va} = G_{1/2O_2(g)}$$
$${}^{\circ}G_{U^{+4}:O^{-2}:O^{-2}} - {}^{\circ}G_{U^{+4}:O^{-2}:Va} = G_{1/2O_2(g)}$$
$${}^{\circ}G_{U^{+5}:O^{-2}:O^{-2}} - {}^{\circ}G_{U^{+5}:O^{-2}:Va} = G_{1/2O_2(g)}$$
$${}^{\circ}G_{U^{+3}:Va:Va} - {}^{\circ}G_{U^{+3}:O^{-2}:Va} = {}^{\circ}G_{U^{+4}:Va:Va} - {}^{\circ}G_{U^{+4}:O^{-2}:Va}$$
$${}^{\circ}G_{U^{+4}:Va:Va} - {}^{\circ}G_{U^{+4}:O^{-2}:Va} = -2\,G_{1/2O_2(g)} + 545210.5$$
$${}^{\circ}G_{U^{+5}:Va:Va} - {}^{\circ}G_{U^{+5}:O^{-2}:Va} = -2\,G_{1/2O_2(g)} + 700000$$
$${}^{\circ}G_{U^{+5}:Va:O^{-2}} = {}^{\circ}G_{U^{+4}:Va:O^{-2}} = {}^{\circ}G_{U^{+3}:Va:O^{-2}} = +100000$$

A few interaction parameters need to be optimized to obtain a good description of the experimental oxygen potential data in $UO_{2\pm x}$ and the phase equilibria data.[100]

We calculate exactly the same phase diagram and oxygen potential data after converting the above parameters into the following six Gibbs energy terms, with a single constituent occupying one specific sublattice and asterisks "*" for the others as follows:

- ${}^{\circ}G_{U^{+4}:*:*} = G_{UO_2}$: the energy of the perfect crystal of UO_2 without defects
- ${}^{\circ}G_{*:*:O^{-2}} = G_{1/2O_2(g)}$: the energy of oxygen incorporating in the third sublattice
- ${}^{\circ}G_{*:Va:*} = -2\ G_{1/2O_2(g)} + 545210.5$: the energy to remove two oxygen atoms in the second sublattice and create oxygen vacancies
- ${}^{\circ}G_{U^{+5}:Va:*} = +700000 - 545210.5 = +154789.5$: this term had to be added to have equivalent terms to the previous model in which a different value had been used for ${}^{\circ}G_{U^{+n}:Va:Va} - {}^{\circ}G_{U^{+n}:O^{-2}:Va}$ when n=5.
- ${}^{\circ}G_{U^{+3}:*:*} = G_{UO_2} + 201916.5 - 70.22618\ T + 1.12467\ RT$ related to the energy to reduce U^{+4} into U^{+3} in UO_2
- ${}^{\circ}G_{U^{+5}:*:*} = G_{UO_2} - 58351.62 + 39.67611T + 0.69315RT$ related to the energy to oxidize U^{+4} into U^{+5} in UO_2 The interaction parameters remain identical.

With this conversion, the number of Gibbs energy terms has been reduced from 12 to 6. This is a promising approach that could be applied to reassess oxide systems that otherwise require the evaluation of many endmembers. Another improvement would be to incorporate the formation energies of point defects (oxygen vacancies and interstitials, as well as U^{+3} and U^{+5}) directly into our model, as these data are well established from calculations with atomic scale methods such as DFT.

4 Conclusions

Computational Thermodynamics (CT), centered around the Calphad methodology, has reached a reliability level so that its tools, i.e., software and databases, are nowadays widely used in academia and industry. At the core of CT is the sublattice model with all of its variants which enables better understanding of existing materials. This has greatly contributed to accelerated design of new materials and the better control of production steps, life cycle performance and recycling, as well as energy efficiency.

The multidimensional Gibbs energy function described as a function of the temperature, pressure and composition makes it possible to calculate all thermodynamic properties, i.e., chemical potentials, heat capacity etc., for each individual phase for any condition, even if the phase is not stable. Such a calculation represents a local equilibrium which is an essential tool for the simulation of phase transitions with kinetic processes such as diffusion, interface reactions, nucleation of other phases etc.

The various types of calculation are possible because the models used within the Calphad method have two very important features: the ability to describe many properties within experimental uncertainty in the area where they are known and the reliability of the extrapolations to higher order systems. Even though FP inputs have contributed significantly to the improvement of the quality of the results obtained from CT and helped to extend its ability to infer properties of multicomponent systems, the strength of CT is demonstrated by the agreement of its calculated results with those from experiments.

This paper details the continuing evolution of the sublattice model to efficiently describe many important cases. It presents perspectives for its future development that expand the limits of its application. The strategy employed by the sublattice model to describe thermodynamic properties can be generally used for the description of molar volume, diffusion mobility and many other phase-based properties.

Today CT is the only reliable method for the calculation of phase equilibria, thermodynamic and phase-based property information in multicomponent, multiphase systems that are comprised of condensed phases with homogeneity ranges.

Acknowledgments One author, SGF acknowledges funding by the Deutsche Forschungsgemeinschaft (DFG) through projects C6 of the collaborative research center SFB/TR 103 (DFG Project Number 190389738) and thanks for the use of the facilities of ZGH (Center for Interface-Dominated High-Performance Materials). The authors are grateful for the knowledgeable comments from an unknown reviewer.

References

1. J.W. Gibbs, On the Equilibrium of Heterogeneous Substances. *Am. J. Sci.*, 1878, 3-16(96): 441-458. https://doi.org/10.2475/ajs.s3-16.96.441.
2. J.J. van Laar, Die Schmelz- oder Erstarrungskurven bei binären Systemen, wenn die feste Phase ein Gemisch (amorphe feste Lösung oder Mischkristalle) der beiden Komponenten ist. *Z. Phys. Chem.*, 1908, 64U(1): 257-297. https://doi.org/10.1515/zpch-1908-6417.
3. H.C. Sorby, On the Microscopical Structure of Iron and Steel. *J. Iron Steel Inst.*, 1887, 1: 255-288.
4. W.C. Roberts-Austen, Fifth Report to the Alloys Research Committee: Steel. In: Proceedings of the Institution of Mechanical Engineers, 1899, 56(1): 35-102. https://doi.org/10.1243/PIME_PROC_1899_056_010_02.
5. H.W. Bakhuis Roozeboom, Eisen und Stahl vom Standpunkte der Phasenlehre. *Zeitschrift für Phys. Chem.*, 1900, 34(1): 437-487. https://doi.org/10.1515/zpch-1900-3429.
6. E. Jänecke, *Summary of Alloys*. Hannover: Dr. Max Jänecke Verlagsbuchhandlung, 1909.
7. M. Hansen, *Der Aufbau der Zweistofflegierungen: Eine kritische Zusammenfassung*. Berlin Heidelberg: Springer, 1936.
8. M. Hansen, R.P. Elliott, and K. Anderko, Constitution of Binary Alloys. In *McGraw-Hill Series in Materials Science and Engineering*. New York: McGraw-Hill, 1958.
9. E. Jänecke, *Kurzgefasstes Handbuch aller Legierungen*. Berlin Heidelberg: Springer, 1937.
10. C. Wagner, *Thermodynamics of Alloys, Vol. 51 of Addison-Wesley Metallurgy Series*. Boston: Addison-Wesley Press, 1952.
11. J.L. Meijering, Calculs Thermodynamiques Concernant la Nature des Zones Guinier-Preston dans les Alliages Aluminium-Cuivre. *Revue de Métall.*, 1952, 49(12): 906-910.
12. J.L. Meijering and H.K. Hardy, Closed Miscibility Gaps in Ternary and Quaternary Regular Alloy Solutions. *Acta Metall.*, 1956, 4(3): 249-256. https://doi.org/10.1016/0001-6160(56)90061-X.
13. J.L. Meijering, Calculation of the Nickel-Chromium-Copper Phase Diagram from Binary Data. *Acta Metall.*, 1957, 5(5): 257-264. https://doi.org/10.1016/0001-6160(57)90099-8.
14. L. Kaufman and A.E. Ringwood, High Pressure Equilibria in the Iron-Nickel System and the Structure of Metallic Meteorites. *Acta Metall.*, 1961, 9(10): 941-944. https://doi.org/10.1016/0001-6160(61)90113-4.
15. L. Kaufman, The Lattice Stability of Metals-I. Titanium and Zirconium. *Acta Metall.*, 1959, 7(8): 575-587. https://doi.org/10.1016/0001-6160(59)90195-6.
16. L. Kaufman, E.V. Clougherty, and R.J. Weiss, The Lattice Stability of Metals-III. Iron. *Acta Metall.*, 1963, 11(5): 323-335. https://doi.org/10.1016/0001-6160(63)90157-3.
17. L. Kaufman, H. Bernstein, Thermodynamic Properties of Refractory Transition Metal Compounds, in: Anisotropy in Single-Crystal Refractory Compounds: Proceedings of an International Symposium on Anisotropy in Single-Crystal Refractory Compounds, held on June 13-15, 1967, in Dayton Ohio. Sponsored by the Ceramics and Branch of the Air Force Materials Laboratory, United States Air Force., Springer, 1968, pp 269-297.
18. O. Kubaschewski and T.G. Chart, Calculation of Metallurgical Equilibrium Diagrams from Thermochemical Data. *J. Inst. Met.*, 1965, 93: 329-338.
19. M. Hillert, Empirical Methods of Predicting and Representing Thermodynamic Properties of Ternary Solution Phases. *Calphad*, 1980, 4(1): 1-12. https://doi.org/10.1016/0364-5916(80)90016-4.
20. P.J. Spencer, A Brief History of Calphad. *Calphad*, 2008, 32(1): 1-8. https://doi.org/10.1016/j.calphad.2007.10.001.
21. M.A. Hillert, Theory of Nucleation for Solid Metallic Solutions, Sc.D. Thesis, Massachusetts Institute of Technology (1956).
22. M. Hillert, A Solid-Solution Model for Inhomogeneous Systems. *Acta Metall.*, 1961, 9(6): 525-535. https://doi.org/10.1016/0001-6160(61)90155-9.
23. J.W. Cahn and J.E. Hilliard, Free Energy of a Nonuniform System. I. Interfacial Free Energy. *J. Chem. Phys.*, 1958, 28(2): 258-267. https://doi.org/10.1063/1.1744102.
24. M. Hillert, On the Nearest Neighbour Interaction Model with a Concentration Dependent Interaction Energy. *J. Phys. Radium*, 1962, 23(10): 835-840. https://doi.org/10.1051/jphysrad:019620023010083500.
25. M.I. Temkin, Mixtures of Fused Salts as Ionic Solutions. *Acta Phys. Chem.*, 1945, 20: 411-420.
26. W. Gorsky, Röntgenographische Untersuchung von Umwandlungen in der Legierung Cu-Au. *Z. Phys.*, 1928, 50(1-2): 64-81. https://doi.org/10.1007/BF01328593.
27. W.L. Bragg, E.J. Williams, The Effect of Thermal Agitation on Atomic Arrangement in Alloys. In: Proceedings of the Royal Society of London. Series A, Containing Papers of a Mathematical and Physical Character 145 (855):699-730. https://doi.org/10.1098/rspa.1934.0132.
28. W. L. Bragg, E. J. Williams The Effect of Thermal Agitation on Atomic Arrangement in Alloys-II. In: Proceedings of the Royal Society of London. Series A - Mathematical and Physical Sciences 151 (874): 540-566 (1935). https://doi.org/10.1098/rspa.1935.0165.
29. E. J. Williams, The Effect of Thermal Agitation on Atomic Arrangement in Alloys-III. In: Proceedings of the Royal Society of London. Series A - Mathematical and Physical Sciences 152 (875):231-252 (1935). https://doi.org/10.1098/rspa.1935.0188.
30. E. A. Guggenheim, The Statistical Mechanics of Regular Solutions. In: Proceedings of the Royal Society of London. Series A - Mathematical and Physical Sciences 148 (864):304-312 (1935). https://doi.org/10.1098/rspa.1935.0020.
31. H. A. Bethe, Statistical Theory of Superlattices, Proceedings of the Royal Society of London. Series A - Mathematical and Physical Sciences, 1935, 150 (871):552-575. https://doi.org/10.1098/rspa.1935.0122.

32. R. Kikuchi, A Theory of Cooperative Phenomena. *Phys. Rev.*, 1951, 81(6): 988-1003. https://doi.org/10.1103/PhysRev.81.988.
33. J. Hijmans and J. De Boer, An Approximation Method for Order-Disorder Problems. *IV Phys.*, 1956, 22(1-5): 408-428. https://doi.org/10.1016/S0031-8914(56)80055-4.
34. C.M. van Baal, Order-Disorder Transformations in a Generalized Ising Alloy. *Physica*, 1973, 64(3): 571-586. https://doi.org/10.1016/0031-8914(73)90010-4.
35. J.M. Sanchez and D. de Fontaine, Ising Model Phase-Diagram Calculations in the fcc Lattice with First- and Second-Neighbor Interactions. *Phys. Rev. B*, 1982, 25(3): 1759-1765. https://doi.org/10.1103/PhysRevB.25.1759.
36. V.L. Moruzzi, J. Janak, and A.R. Williams, *Calculated Electronic Properties of Metals*. Oxford: Pergamon Press, 1978.
37. J.W.D. Connolly and A.R. Williams, Density-Functional Theory Applied to Phase Transformations in Transition-Metal Alloys. *Phys. Rev. B*, 1983, 27(8): 5169-5172. https://doi.org/10.1103/PhysRevB.27.5169.
38. K. Terakura, T. Oguchi, T. Mohri, and K. Watanabe, Electronic Theory of the Alloy Phase Stability of Cu-Ag, Cu-Au, and Ag-Au Systems. *Phys. Rev. B*, 1987, 35(5): 2169-2173. https://doi.org/10.1103/PhysRevB.35.2169.
39. S.-H. Wei, A.A. Mbaye, L.G. Ferreira, and A. Zunger, First-Principles Calculations of the Phase Diagrams of Noble Metals: Cu-Au, Cu-Ag, and Ag-Au. *Phys. Rev. B*, 1987, 36(8): 4163-4185. https://doi.org/10.1103/PhysRevB.36.4163.
40. M. Sluiter, D. de Fontaine, X.Q. Guo, R. Podloucky, and A.J. Freeman, First-Principles Calculation of Phase Equilibria in the Aluminum Lithium System. *Phys. Rev. B*, 1990, 42(16): 10460-10476. https://doi.org/10.1103/PhysRevB.42.10460.
41. M. Hillert and L.I. Staffansson, Regular-Solution Model for Stoichiometric Phases and Ionic Melts. *Acta Chem. Scand.*, 1970, 24(10): 3618-3626. https://doi.org/10.3891/acta.chem.scand.24-3618.
42. M. Hillert, The Compound Energy Formalism. *J. Alloy. Compd.*, 2001, 320(2): 161-176. https://doi.org/10.1016/S0925-8388(00)01481-X.
43. B. Sundman and J. Ågren, A Regular Solution Model for Phases with Several Components and Sublattices, Suitable for Computer Applications. *J. Phys. Chem. Solids*, 1981, 42(4): 297-301. https://doi.org/10.1016/0022-3697(81)90144-X.
44. R. Podloucky, H.J.F. Jansen, X.Q. Guo, and A.J. Freeman, First-Principles Electronic-Structure Approach for Phase Diagrams of Binary Alloys. *Phys. Rev. B*, 1988, 37: 5478-5482. https://doi.org/10.1103/PhysRevB.37.5478.
45. M.H.F. Sluiter, K. Esfarjani, and Y. Kawazoe, Site Occupation Reversal in the Fe-Cr σ Phase. *Phys. Rev. Lett.*, 1995, 75(17): 3142-3145. https://doi.org/10.1103/PhysRevLett.75.3142.
46. A. Van De Walle, M. Asta, and G. Ceder, The Alloy Theoretic Automated Toolkit: A User Guide. *Calphad*, 2002, 26(4): 539-553. https://doi.org/10.1016/S0364-5916(02)80006-2.
47. M.H.F. Sluiter and Y. Kawazoe, Invariance of Truncated Cluster Expansions for First-Principles Alloy Thermodynamics. *Phys. Rev. B*, 2005, 71(21): 212201. https://doi.org/10.1103/PhysRevB.71.212201.
48. D. de Fontaine, Cluster Approach to Order-Disorder Transformations in Alloys. In *Solid State Physics*, 1994, 33-176. Amsterdam: Elsevier.
49. M. Enoki, B. Sundman, M.H.F. Sluiter, M. Selleby, and H. Ohtani, Calphad Modeling of LRO and SRO Using ab Initio Data. *Metals*, 2020, 10(8): 998. https://doi.org/10.3390/met10080998.
50. S. Tumminello, M. Palumbo, J. Koßmann, T. Hammerschmidt, P.R. Alonso, S. Sommadossi, and S.G. Fries, DFT-CEF Approach for the Thermodynamic Properties and Volume of Stable and Metastable Al-Ni Compounds. *Metals*, 2020, 10(9): 1142. https://doi.org/10.3390/met10091142.
51. P.D. Tepesch, M. Asta, and G. Ceder, Computation of Configurational Entropy Using Monte Carlo Probabilities in Cluster-Variation Method Entropy Expressions. *Modell. Simul. Mater. Sci. Eng.*, 1998, 6(6): 787-797. https://doi.org/10.1088/0965-0393/6/6/009.
52. C. Colinet, Applications of the Cluster Variation Method to Empirical Phase Diagram Calculations. *Calphad*, 2001, 25(4): 607-623. https://doi.org/10.1016/S0364-5916(02)00011-1.
53. X. Zhang and M.H.F. Sluiter, Cluster Expansions for Thermodynamics and Kinetics of Multicomponent Alloys. *J. Phase Equilib. Diffus.*, 2016, 37: 44-52. https://doi.org/10.1007/s11669-015-0427-x.
54. N. Dupin, U.R. Kattner, B. Sundman, M. Palumbo, and S.G. Fries, Implementation of an Effective Bond Energy Formalism in the Multicomponent Calphad Approach. *J. Res. Nat. Inst. Stand. Technol.*, 2018, 123: 1-33. https://doi.org/10.6028/jres.123.020.
55. G. Kirchner, T. Nishizawa, and B. Uhrenius, The Distribution of Chromium Between Ferrite and Austenite and the Thermodynamics of the α/γ Equilibrium in the Fe-Cr and Fe-Mn Systems. *Metall. Trans.*, 1973, 4: 167-174. https://doi.org/10.1007/BF02649616.
56. M. Hillert and M. Waldenström, A Thermodynamic Analysis of the Fe-Mn-C System. *Metall. Trans. A*, 1977, 8A: 5-13. https://doi.org/10.1007/BF02677257.
57. A. Fernández Guillermet, M. Hillert, B. Jansson, and B. Sundman, An Assessment of the Fe-S System Using a Two-Sublattice Model for the Liquid Phase. *Metall. Trans. B*, 1981, 12: 745-754. https://doi.org/10.1007/BF02654144.
58. S. Hertzman and B. Sundman, A Thermodynamic Analysis of the Fe-Cr System. *Calphad*, 1982, 6: 67-80. https://doi.org/10.1016/0364-5916(82)90018-9.
59. G. Inden, Approximate Description of the Configurational Specific Heat During a Magnetic Order-Disorder Transformation. In: Proceedings Calphad V, Düsseldorf, 1976, pp III. 4-1-13.
60. G. Inden, The Role of Magnetism in the Calculation of Phase Diagrams. *Phys. B*, 1981, 103: 82-100. https://doi.org/10.1016/0378-4363(81)91004-4.
61. M. Hillert, Some Viewpoints on the Use of a Computer for Calculating Phase Diagrams. *Phys. B*, 1981, 103: 31-40. https://doi.org/10.1016/0378-4363(81)91000-7.
62. B. Jansson, Computer Operated Methods for Equilibrium Calculations and Evaluation of Thermochemical Model Parameters, Ph.D. thesis, KTH, Royal Institute of Technology (1984).
63. B. Sundman, Application of Computer Techniques on the Treatment of the Thermodynamics of Alloys, Ph.D. thesis, KTH, Royal Institute of Technology (1981).
64. J.-O. Andersson, T. Helander, L. Höglund, P. Shi, and B. Sundman, Thermo-Calc and DICTRA, Computational Tools for Materials Science. *Calphad*, 2002, 26(2): 273-312. https://doi.org/10.1016/S0364-5916(02)00037-8.
65. L. Kaufman and H. Bernstein, *Computer Calculation of Phase Diagrams*. New York: With Special Reference to Refractory Metals Academic Press, 1970.
66. A.T. Dinsdale, SGTE Data for Pure Elements. *Calphad*, 1991, 15: 317-425. https://doi.org/10.1016/0364-5916(91)90030-N.
67. M. Hillert and M. Jarl, A Model for Alloying in Ferromagnetic Metals. *Calphad*, 1978, 2(3): 227-238. https://doi.org/10.1016/0364-5916(78)90011-1.
68. B. Sundman, B. Jansson, and J.-O. Andersson, The Thermo-Calc Databank System. *Calphad*, 1985, 9: 153-190. https://doi.org/10.1016/0364-5916(85)90021-5.

69. Q. Chen and B. Sundman, Modeling of Thermodynamic Properties for bcc, fcc, Liquid, and Amorphous Iron. *J. Phase Equilib.*, 2001, 22(6): 631-644. https://doi.org/10.1361/105497101770332442.
70. Z. He, F. Haglöf, Q. Chen, A. Blomqvist, and M. Selleby, A Third Generation Calphad Description of Fe: Revisions of fcc, hcp and Liquid. *J. Phase Equilib. Diffus.*, 2022, 43(3): 287-303. https://doi.org/10.1007/s11669-022-00961-w.
71. B. Sundman and F. Aldinger, The Ringberg Workshop 1995 on Unary Data for Elements and Other End-Members of Solutions. *Calphad*, 1995, 19(4): 433-436. https://doi.org/10.1016/0364-5916(96)00001-6.
72. H. Kopp, Investigation of the Specific Heats of Solid Bodies. *Philos. Trans. R. Soc. London*, 1865, 155: 71-202. https://doi.org/10.1098/rstl.1865.0003.
73. L. Kaufman and J. Ågren, CALPHAD, First and Second Generation - Birth of the Materials Genome. *Scripta Mater.*, 2014, 70: 3-6. https://doi.org/10.1016/j.scriptamat.2012.12.003.
74. J. Ågren, Thermodynamics of Supercooled Liquids and Their Glass Transition. *Phys. Chem. Liq.*, 1988. https://doi.org/10.1080/00319108808078586.
75. C.A. Becker, J. Ågren, M. Baricco, Q. Chen, S.A. Decterov, U.R. Kattner, J.H. Perepezko, G.R. Pottlacher, and M. Selleby, Thermodynamic Modelling of Liquids: Calphad Approaches and Contributions from Statistical Physics. *Phys. Status Solidi (B) Basic Res.*, 2014, 251(1): 33-52. https://doi.org/10.1002/pssb.201350149.
76. Z. He, B. Kaplan, H. Mao, and M. Selleby, The Third Generation Calphad Description of Al-C Including Revisions of Pure Al and C. *Calphad*, 2021, 72: 102250. https://doi.org/10.1016/j.calphad.2021.102250.
77. B. Sundman, U.R. Kattner, M. Hillert, M. Selleby, J. Ågren, S. Bigdeli, Q. Chen, A. Dinsdale, B. Hallstedt, A. Khvan, H. Mao, and R.A. Otis, A Method for Handling the Extrapolation of Solid Crystalline Phases to Temperatures Far Above Their Melting Point. *Calphad Comput. Coupling Phase Diagr. Thermochem.*, 2020, 68: 101737. https://doi.org/10.1016/j.calphad.2020.101737.
78. R. Schmid-Fetzer, Third Generation of Unary Calphad Descriptions and the Avoidance of Re-Stabilized Solid Phases and Unexpected Large Heat Capacity. *J. Phase Equilib. Diffus.*, 2022, 43(3): 304-316. https://doi.org/10.1007/S11669-022-00976-3.
79. S. Bigdeli, L.-F. Zhu, A. Glensk, B. Grabowski, B. Lindahl, T. Hickel, and M. Selleby, An Insight Into Using DFT Data for Calphad Modeling of Solid Phases in the Third Generation of Calphad Databases, a Case Study for Al. *Calphad*, 2019, 65: 79-85. https://doi.org/10.1016/j.calphad.2019.02.008.
80. W. Xiong, Q. Chen, P.A. Korzhavyi, and M. Selleby, CALPHAD: Computer Coupling of Phase Diagrams and Thermochemistry An Improved Magnetic Model for Thermodynamic Modeling. *Calphad*, 2012, 39: 11-20.
81. M. Selleby, Z. He, Third Generation Calphad for Elements - Model Discussion with Hands-on Instructions and Examples, Journal of Phase Equilibria and Diffusion 45 (2024) this issue.
82. B. Sundman, An Assessment of the Fe-O System. *J. Phase Equilib.*, 1991, 12(2): 127-140. https://doi.org/10.1007/BF02645709.
83. I. Ansara and B. Sundman, Calculation of the Magnetic Contribution for Intermetallic Compounds. *Calphad*, 2000, 24: 181-182. https://doi.org/10.1016/S0364-5916(00)00022-5.
84. X.-G. Lu, M. Selleby, and B. Sundman, Implementation of a New Model for Pressure Dependence of Condenced Phases in Thermo-Calc. *Calphad*, 2005. https://doi.org/10.1016/j.calphad.2005.04.001.
85. M. Hillert, Empirical Methods of Predicting and Representing Thermodynamic Properties of Ternary Solution Phases. *Calphad*, 1980, 4: 1-12. https://doi.org/10.1016/0364-5916(80)90016-4.
86. O. Redlich and A.T. Kister, Algebraic Representation of Thermodynamic Properties and the Classification of Solutions. *Ind. Eng. Chem.*, 1948, 40: 345-348. https://doi.org/10.1021/ie50458a036.
87. M. Hillert and B. Sundman, Predicting Miscibility Gaps in Reciprocal Liquids. *Calphad*, 2001, 25: 599-605. https://doi.org/10.1016/S0364-5916(02)00010-X.
88. B. Sundman, X.-G. Lu, and H. Ohtani, The Implementation of an Algorithm to Calculate Thermodynamic Equilibria for Multi-Component Systems with Non-Ideal Phases in a Free Software. *Comput. Mater. Sci.*, 2015, 101: 127-137. https://doi.org/10.1016/j.commatsci.2015.01.029.
89. A. Zunger, S.H. Wei, L.G. Ferreira, and J.E. Bernard, Special Quasirandom Structures. *Phys. Rev. Lett.*, 1990, 65: 353. https://doi.org/10.1103/PhysRevLett.65.353.
90. P. Gustafson, A Thermodynamic Evaluation of the C-Fe-W System. *Metall. Trans. A*, 1987, 18A(2): 175-188. https://doi.org/10.1007/BF02825699.
91. A. Gabriel, P. Gustafson, and I. Ansara, A Thermodynamic Evaluation of the C-Fe-Ni System. *Calphad*, 1987, 11(3): 203-218. https://doi.org/10.1016/0364-5916(87)90039-3.
92. J.-O. Andersson, A Thermodynamic Evaluation of the Fe-Cr-C System. *Metall. Trans. A*, 1988, 19A: 627-636. https://doi.org/10.1007/BF02649276.
93. W. Huang, A Thermodynamic Assessment of the Fe-Mn-C System. *Metall. Trans. A*, 1990, 21(8A): 2115-2123. https://doi.org/10.1007/BF02647870.
94. C. Qiu, An Analysis of the Cr-Fe-Mo-C System and Modification of Thermodynamic Parameters. *ISIJ Int.*, 1992, 32(10): 1117-1127. https://doi.org/10.2355/isijinternational.32.1117.
95. B.-J. Lee, A Thermodynamic Evaluation of the Fe-Cr-Mn-C System. *Metall. Trans. A*, 1993, 24A(5): 1017-1025. https://doi.org/10.1007/BF02657232.
96. P. Gustafson, A Thermodynamic Evaluation of the Fe-C System. *Scand. J. Metall.*, 1985, 14: 259-267.
97. J.-O. Andersson, Thermodynamic Properties of Mo-C. *Calphad*, 1988, 12(1): 1-8. https://doi.org/10.1016/0364-5916(88)90024-7.
98. J.-O. Andersson, Thermodynamic Evaluation of the Fe-Mo-C System. *Calphad*, 1988, 12(1): 8-23. https://doi.org/10.1016/0364-5916(88)90025-9.
99. P. Liang, N. Dupin, S.G. Fries, H. Seifert, I. Ansara, H. Lukas, and F. Aldinger, Thermodynamic Assessment of the Zr-O Binary System. *Z. Metallkd.*, 2001, 92(7): 747-756. https://doi.org/10.1515/ijmr-2001-0140.
100. C. Guéneau, N. Dupin, B. Sundman, C. Martial, J.-C. Dumas, S. Gossé, S. Chatain, F. de Bruycker, D. Manara, and R.J.M. Konings, Thermodynamic Modelling of Advanced Oxide and Carbide Nuclear Fuels: Description of the U-Pu-O-C Systems. *J. Nucl. Mater.*, 2011, 419(1-3): 145-167. https://doi.org/10.1016/j.jnucmat.2011.07.033.
101. V. Eremenko, T. Velinakova, A. Khar'kova, and A. Bondar, Equilibrium Diagrams of Ternary Systems of Rhenium with Carbon and Transition Metals of Group iii-vii of the Periodic System iof the Elements. *Poroshkovaya Metall.*, 1989, 10(322): 62-69.
102. J.-O. Andersson and B. Sundman, Thermodynamic Properties of the Cr-Fe System. *Calphad*, 1987, 11(1): 83-92. https://doi.org/10.1016/0364-5916(87)90021-6.
103. I. Ansara, T.G. Chart, A. Fernández Guillermet, P.C. Hayes, U.R. Kattner, D.G. Pettifor, N. Saunders, and K. Zeng, Thermodynamic Modelling of Selected Topologically Close-Packed

Intermetallic Compounds. *Calphad*, 1997, 21(2): 171-218. https://doi.org/10.1016/S0364-5916(97)00021-7.
104. M. Hillert and C. Qiu, A Reassessment of the Cr-Fe-Ni System. *Metall. Trans. A*, 1990, 21A: 1673-1680. https://doi.org/10.1007/BF02672583.
105. C.A. Coughanowr, I. Ansara, R. Luoma, M. Hämäläinen, and H.L. Lukas, Assessment of the Cu-Mg System. *Z. Met.*, 1991, 82(7): 574-581. https://doi.org/10.1515/ijmr-1991-820711.
106. J.G. Costa Neto, S.G. Fries, H.L. Lukas, S. Gama, and G. Effenberg, Thermodynamic Optimisation of the Nb-Cr System. *Calphad*, 1993, 17(3): 219-228. https://doi.org/10.1016/0364-5916(93)90001-R.
107. B. Sundman, U.R. Kattner, M. Palumbo, and S.G. Fries, OpenCalphad - A Free Thermodynamic Software. *Integr. Mater. Manuf. Innov.*, 2015, 4: 1-15. https://doi.org/10.1186/s40192-014-0029-1.
108. I. Ansara, B. Sundman, and P. Willemin, Thermodynamic Modeling of Ordered Phases in the Ni-Al System. *Acta Metall.*, 1988, 36(4): 977-982. https://doi.org/10.1016/0001-6160(88)90152-6.
109. J. Lacaze and B. Sundman, An Assessment of the Fe-C-Si System. *Metall. Trans. A*, 1991, 22A: 2211-2223. https://doi.org/10.1007/BF02664987.
110. M.H.F. Sluiter, Ab Initio Lattice Stabilities of Some Elemental Complex Structures. *Calphad*, 2006, 30(4): 357-366. https://doi.org/10.1016/j.calphad.2006.09.002.
111. M.H.F. Sluiter, Lattice Stability Prediction of Elemental Tetrahedrally Close-Packed Structures. *Acta Mater.*, 2007, 55(11): 3707-3718. https://doi.org/10.1016/j.actamat.2007.02.016.
112. J.F. Martin, F. Müller, and O. Kubaschewski, Thermodynamic Properties of $TaCr_2$ and $NbCr_2$. *Trans. Faraday Soc.*, 1970, 66: 1065-1072. https://doi.org/10.1039/TF9706601065.
113. A. Ormeci, F. Chu, J.M. Wills, T.E. Mitchell, R.C. Albers, D.J. Thoma, and S.P. Chen, Total-Energy Study of Electronic Structure and Mechanical Behavior of C15 Laves Phase Compounds: $NbCr_2$ and HfV_2. *Phys. Rev. B*, 1996, 54(18): 12753-12762. https://doi.org/10.1103/PhysRevB.54.12753.
114. S. Hong and C.L. Fu, Phase Stability and Elastic Moduli of Cr_2Nb by First-Principles Calculations. *Intermetallics*, 1999, 7(1): 5-9. https://doi.org/10.1016/S0966-9795(98)00005-3.
115. A. Kellou, T. Grosdidier, C. Coddet, and H. Aourag, Theoretical Study of Structural, Electronic, and Thermal Properties of Cr_2(Zr, Nb) Laves Alloys. *Acta Mater.*, 2005, 53(5): 1459-1466. https://doi.org/10.1016/j.actamat.2004.11.039.
116. Q. Yao, J. Sun, Y. Zhang, and B. Jiang, First-Principles Studies of Ternary Site Occupancy in the C15 $NbCr_2$ Laves Phase. *Acta Mater.*, 2006, 54(13): 3585-3591. https://doi.org/10.1016/j.actamat.2006.03.039.
117. J. Pavlů, J. Vřešťál, and M. Šob, Re-Modeling of Laves Phases in the Cr-Nb and Cr-Ta Systems Using First-Principles Results. *Calphad*, 2009, 33(1): 179-186. https://doi.org/10.1016/j.calphad.2008.04.006.
118. C. Schmetterer, A.V. Khvan, A. Jacob, B. Hallstedt, and T. Markus, A New Theoretical Study of the Cr-Nb System. *J. Phase Equilib. Diffus.*, 2014, 35(4): 434-444. https://doi.org/10.1007/s11669-014-0313-y.
119. H.-J. Lu, W.-B. Wang, N. Zou, J.-Y. Shen, X.-G. Lu, and Y. He, Thermodynamic Modeling of Cr-Nb and Zr-Cr with Extension to the Ternary Zr-Nb-Cr System. *Calphad*, 2015, 50: 134-143. https://doi.org/10.1016/j.calphad.2015.06.002.
120. S.G. Fries and B. Sundman, Using Re-W σ-Phase First-Principles Results in the Bragg-Williams Approximation to Calculate Finite-Temperature Thermodynamic Properties. *Phys. Rev. B*, 2002, 66: 012203. https://doi.org/10.1103/PhysRevB.66.012203.
121. N. Dupin, S.G. Fries, J.-M. Joubert, B. Sundman, M.H.F. Sluiter, Y. Kawazoe, and A. Pasturel, Using First-Principles Results to Calculate Finite-Temperature Thermodynamic Properties of the Nb-Ni μ Phase in the Bragg-Williams Approximation. *Phil. Mag.*, 2006, 86(12): 1631-1641. https://doi.org/10.1080/14786430500437488.
122. B. Hallstedt and M. Noori, Hybrid Calphad DFT Modelling of the Mg-Al-Ca System. *Calphad*, 2023, 82: 102577. https://doi.org/10.1016/j.calphad.2023.102577.
123. R. Mathieu, N. Dupin, J.-C. Crivello, K. Yaqoob, A. Breidi, J.-M. Fiorani, N. David, and J.-M. Joubert, CALPHAD Description of the Mo-Re System Focused on the Sigma Phase Modeling. *Calphad*, 2013, 43: 18-31. https://doi.org/10.1016/j.calphad.2013.08.002.
124. J.C. Pereira dos Santos, S. Griesemer, N. Dupin, U.R. Kattner, C. Liu, D. Ivanova, T. Hammerschmidt, S.G. Fries, C. Wolverton, and C.E. Campbell, Applying the Effective Bond Energy Formalism (EBEF) to Describe the Sigma (σ) Phase in the Co-Cr-Ni-Re System. *J. Phase Equilib. Diffus.*, 2023.https://doi.org/10.1007/s11669-023-01079-3.
125. L. Dumitrescu and B. Sundman, A Thermodynamic Reassessment of the Si-Al-O-N System. *J. Eur. Ceram. Soc.*, 1995, 15(3): 239-247. https://doi.org/10.1016/0955-2219(95)93945-Y.
126. M. Hillert and B. Jansson, Thermodynamic Model for Nonstoichiometric Ionic Phases - Application to CeO_{2-x}. *J. Am. Ceram. Soc.*, 1986, 69(10): 732-734. https://doi.org/10.1111/j.1151-2916.1986.tb07334.x.
127. M. Hillert, B. Jansson, and B. Sundman, Application of the Compound-Energy Model to Oxide Systems. *Z. Met.*, 1988, 79(2): 81-87. https://doi.org/10.1515/ijmr-1988-790203.
128. T.I. Barry, A.T. Dinsdale, J.A. Gisby, B. Hallstedt, M. Hillert, B. Jansson, S. Jonsson, B. Sundman, and J.R. Taylor, The Compound Energy Model for Ionic Solutions with Applications to Solid Oxides. *J. Phase Equilib.*, 1992, 13(5): 459-475. https://doi.org/10.1007/BF02665760.
129. S.A. Degterov, A.D. Pelton, H.J. Seifert, O.B. Fabrichnaya, J.P. Hajra, A. Navrotsky, K. Helean, V. Swamy, A. Costa Silva, and P.J. Spencer, Thermodynamic Modelling of Oxide and Oxynitride Phases. *Zeitschrift für Metall.*, 2001, 92(6): 533-549. https://doi.org/10.3139/ijmr-2001-0107.
130. A.N. Grundy, B. Hallstedt, and L.J. Gauckler, Experimental Phase Diagram Determination and Thermodynamic Assessment of the La_2O_3-SrO System. *Acta Mater.*, 2002, 50(9): 2209-2222. https://doi.org/10.1016/S1359-6454(01)00432-3.
131. J.A. Kilner and M. Burriel, Materials for Intermediate-Temperature Solid-Oxide Fuel Cells. *Annu. Rev. Mater. Res.*, 2014, 44(1): 365-393. https://doi.org/10.1146/annurev-matsci-070813-113426.
132. A.N. Grundy, M. Chen, B. Hallstedt, and L.J. Gauckler, Assessment of the La-Mn-O System. *J. Phase Equilib. Diffus.*, 2005, 26(2): 131-151. https://doi.org/10.1361/15477030523021.
133. A.N. Grundy, B. Hallstedt, and L.J. Gauckler, Assessment of the La-Sr-Mn-O System. *Calphad*, 2004, 28(2): 191-201. https://doi.org/10.1016/j.calphad.2004.07.001.
134. A.N. Grundy, E. Povoden, T. Ivas, and L.J. Gauckler, Calculation of Defect Chemistry Using the CALPHAD Approach. *Calphad*, 2006, 30(1): 33-41. https://doi.org/10.1016/j.calphad.2005.11.004.
135. J. Mizusaki, N. Mori, H. Takai, Y. Yonemura, H. Minamiue, H. Tagawa, M. Dokiya, H. Inaba, K. Naraya, T. Sasamoto, and T. Hashimoto, Oxygen Nonstoichiometry and Defect Equilibrium in the Perovskite-Type Oxides $La_{1-x}Sr_xMnO_{3+\delta}$. *Solid State Ionics*, 2000, 129(1): 163-177. https://doi.org/10.1016/S0167-2738(99)00323-9.
136. J.A. Alonso, Non-stoichiometry and Properties of Mixed-Valence Manganites. *Philos. Trans. R. Soc. London Ser. A Math. Phys. Sci.*, 1998, 356(1742): 1617-1634. https://doi.org/10.1098/rsta.1998.0238.

137. D. Djurovic, M. Zinkevich, and F. Aldinger, Thermodynamic Modeling of the Cerium-Yttrium-Oxygen System. *Solid State Ionics*, 2008, 179(33-34): 1902-1911. https://doi.org/10.1016/j.ssi.2008.06.011.
138. C. Guéneau, M. Baichi, D. Labroche, C. Chatillon, and B. Sundman, Thermodynamic Assessment of the Uranium-Oxygen System. *J. Nucl. Mater.*, 2002, 304(2-3): 161-175. https://doi.org/10.1016/S0022-3115(02)00878-4.
139. B. Hallstedt, Thermodynamic Assessment of the System MgO-Al_2O_3. *J. Am. Ceram. Soc.*, 1992, 75(6): 1497-1507. https://doi.org/10.1111/j.1151-2916.1992.tb04216.x.
140. Q. Chen and M. Hillert, The Compound Energy Model for Compound Semiconductors. *J. Alloy. Compd.*, 1996, 245(1-2): 125-131. https://doi.org/10.1016/S0925-8388(96)02441-3.
141. Q. Chen, M. Hillert, B. Sundman, W.A. Oates, S.G. Fries, and R. Schmid-Fetzer, Phase Equilibria, Defect Chemistry and Semiconducting Properties of CdTe(s)–Thermodynamic Modeling. *J. Electron. Mater.*, 1998, 27(8): 961-971. https://doi.org/10.1007/s11664-998-0128-x.
142. A.S. Jordan, A Review of Semiconductor Phase Diagram Calculations Employing the Regular Associated Solution (RAS) Model. In *Calculation of Phase Diagrams and Thermochemistry of Alloys*, ed. Y. Chang and F. Smith, 1979, 100-129. TMS-AIME.
143. F. Sommer, Alloy Phase Diagrams. In: MRS Symposium Proceedings, 1983, 19: 163-173.
144. R. Schmid and Y.A. Chang, A Thermodynamic Study on an Associated Solution Model for Liquids Alloys. *Calphad*, 1985, 9: 363-382. https://doi.org/10.1016/0364-5916(85)90004-5.
145. A.D. Pelton and M. Blander, Thermodynamic Analysis of Ordered Liquid Solutions by a Modified Quasichemical Approach-Application to Silicate Slags. *Metall. Trans. B*, 1986, 17B: 805-815. https://doi.org/10.1007/BF02657144.
146. A.D. Pelton, P. Chartrand, and G. Eriksson, The Modified Quasi-Chemical Model: Part IV. *Two-Sublattice Quadruplet Approx. Metall. Mater. Trans. A*, 2001, 32A: 1409-1416. https://doi.org/10.1007/s11661-001-0230-7.
147. M. Hillert, B. Jansson, B. Sundman, and J. Ågren, A Two-Sublattice Model for Molten Solutions with Different Tendency for Ionization. *Metall. Trans. A*, 1985, 16A: 261-266. https://doi.org/10.1007/BF02816052.
148. H.L. Lukas, S.G. Fries, and B. Sundman, Computational Thermodynamics. In *The CALPHAD Method*. Cambridge UK: Cambridge University Press, 2007.
149. M. Selleby, An Assessment of the Ca-Fe-O-Si System. *Metall. Mater. Trans. B.*, 1997, 28B: 577-597. https://doi.org/10.1007/s11663-997-0030-6.
150. M. Hillert, L. Kjellqvist, H. Mao, M. Selleby, and B. Sundman, Parameters in the Compound Energy Formalism for Ionic Systems. *Calphad*, 2009, 33: 227-232. https://doi.org/10.1016/j.calphad.2008.05.006.
151. W. Shockley, Theory of Order for the Copper Gold Alloy System. *J. Chem. Phys.*, 1938, 6(3): 130-144. https://doi.org/10.1063/1.1750214.
152. B. Sundman, S.G. Fries, and W.A. Oates, A Thermodynamic Assessment of the Au-Cu System. *Calphad*, 1998, 22(3): 335-354. https://doi.org/10.1016/S0364-5916(98)00034-0.
153. A. Kusoffsky, N. Dupin, and B. Sundman, On the Compound Energy Formalism Applied to fcc Ordering. *Calphad*, 2001, 25(4): 549-565. https://doi.org/10.1016/S0364-5916(02)00007-X.
154. T. Abe and B. Sundman, A Description of the Effect of Short Range Ordering in the Compound Energy Formalism. *Calphad*, 2003, 27(4): 403-408. https://doi.org/10.1016/j.calphad.2004.01.005.
155. P. Franke, An Assessment of the Ordered Phases in Mn-Ni Using Two-and Four-Sublattice Models. *Int. J. Mater. Res.*, 2007, 98(10): 954-960. https://doi.org/10.3139/146.101558.
156. X.-G. Lu, B. Sundman, and J. Ågren, Thermodynamic Assessments of the Ni-Pt and Al-Ni-Pt Systems. *Calphad*, 2009, 33(3): 450-456. https://doi.org/10.1016/j.calphad.2009.06.002.
157. T. Abe and M. Shimono, A Description of the Effect of Short-Range Ordering in BCC Phases with Four Sublattices. *Calphad*, 2014, 45: 40-48. https://doi.org/10.1016/j.calphad.2013.11.006.
158. W. Zheng, S. He, M. Selleby, Y. He, L. Li, X.-G. Lu, and J. Ågren, Thermodynamic Assessment of the Al-C-Fe System. *Calphad*, 2017, 58: 34-49. https://doi.org/10.1016/j.calphad.2017.05.003.
159. Y. Liu, B. Sundman, Y. Du, J. Wang, S. Liu, W.P. Gong, and C. Zhang, A Stepwise Thermodynamic Modeling of the Phase Diagram for the Cu-Be System. *J. Mater. Sci.*, 2018, 53(5): 3756-3766. https://doi.org/10.1007/s10853-017-1777-z.
160. I. Ohnuma, S. Shimenouchi, T. Omori, K. Ishida, and R. Kainuma, Experimental Determination and Thermodynamic Evaluation of Low-Temperature Phase Equilibria in the Fe-Ni Binary System. *Calphad*, 2019, 67: 101677. https://doi.org/10.1016/j.calphad.2019.101677.
161. N. Dupin and B. Sundman, A Thermodynamic Database for Ni-base Superalloys. *Scand. J. Metall.*, 2001, 30(3): 184-192. https://doi.org/10.1034/j.1600-0692.2001.300309.x.
162. J. Bratberg, H. Mao, L. Kjellqvist, A. Engström, P. Mason, and Q. Chen, The Development and Validation of a New Thermodynamic Database for Ni-Based Alloys. *Superalloys*, 2012, 2012(12): 803-812. https://doi.org/10.1002/9781118516430.ch89.
163. H.-L. Chen, H. Mao, and Q. Chen, Database Development and Calphad Calculations for High Entropy Alloys: Challenges, Strategies, and Tips. *Mater. Chem. Phys.*, 2017.https://doi.org/10.1016/j.matchemphys.2017.07.082.
164. H. Mao, H.-L. Chen, and Q. Chen, TCHEA1: A Thermodynamic Database Not Limited for High Entropy Alloys. *J. Phase Equilib. Diffus.*, 2017, 38: 353-368. https://doi.org/10.1007/s11669-017-0570-7.
165. N. Dupin, Contribution à l'évaluation Thermodynamique des Alliages Polyconstitués à Base de Nickel, Ph.D. thesis, Grenoble INPG,1995.
166. I. Ansara, N. Dupin, H.L. Lukas, and B. Sundman, Thermodynamic Assessment of the Al-Ni System. *J. Alloy. Compd.*, 1997, 247(1-2): 20-30. https://doi.org/10.1016/S0925-8388(96)02652-7.
167. I. Ansara, N. Dupin, and B. Sundman, Reply to the Paper: "When is a Compound Energy Not a Compound Energy? A Critique of the 2-Sublattice Order/Disorder Model" of Nigel Saunders. *Calphad*, 1996, 20: 491-499.
168. B. Hallstedt, N. Dupin, M. Hillert, L. Höglund, H.L. Lukas, J.C. Schuster, and N. Solak, Thermodynamic Models for Crystalline Phases. Composition Dependent Models for Volume, Bulk Modulus and Thermal Expansion. *Calphad*, 2007, 31(1): 28-37. https://doi.org/10.1016/j.calphad.2006.02.008.
169. B. Sundman, I. Ohnuma, N. Dupin, U.R. Kattner, and S.G. Fries, An Assessment of the Entire Al-Fe System Including $D0_3$ Ordering. *Acta Mater.*, 2009, 57(10): 2896-2908. https://doi.org/10.1016/j.actamat.2009.02.046.
170. M. Palm and J. Lacaze, Assessment of the Al-Fe-Ti System. *Intermetallics*, 2006, 14(10): 1291-1303. EUROMAT, European Congress on Advanced Materials and Processes, 2005. https://doi.org/10.1016/j.intermet.2005.11.026.
171. Z. Liang, U. Kattner, K. Choudharry, F. Tavazza, and C. Campbell, Thermodynamic Assessments of Ti-Al, Ti-Fe, and Ti-Al-Fe Systems with 4 Sublattice Description of Ordered BCC

Phase and DFT Data. *J. Phase Equilib. Diffus.*, 2024. https://doi.org/10.1007/s11669-024-01124-9.
172. W.A. Oates, P.J. Spencer, and S.G. Fries, A Cluster Expansion for Cu-Au Alloys Based on Experimental Data. *Calphad*, 1996, 20(4): 481-489. https://doi.org/10.1016/S0364-5916(97)00010-2.
173. I. Ansara, B. Burton, Q. Chen, M. Hillert, A. Fernández Guillermet, S.G. Fries, H.L. Lukas, H.-J. Seifert, and W.A. Oates, Models for Composition Dependence. *Calphad*, 2000, 24(1): 19-40. https://doi.org/10.1016/S0364-5916(00)00013-4.
174. A. Breidi, M. Andasmas, J.C. Crivello, N. Dupin, and J.M. Joubert, Experimental and Computed Phase Diagrams of the Fe-Re System. *J. Phys. Condens. Matter*, 2014, 26(48): 485402. https://doi.org/10.1088/0953-8984/26/48/485402.
175. T. Oliphant, Guide to NumPy, 2006. https://web.mit.edu/dvp/Public/numpybook.pdf, visited 23-Jul-2024.
176. D. Ivanova, Thermodynamic Modeling of the Mo-Ni-Re σ Phase by the Effective Bond Energy Formalism, Student Project Report, Ruhr University Bochum, Bochum, Germany, 2019.
177. B. Sundman, C. Guéneau, and N. Dupin, Modeling Multiple Defects in Ionic Phases Like $UO_{2\pm x}$ Using the Compound Energy Formalism. *Acta Mater.*, 2011, 59: 6039-6047. https://doi.org/10.1016/j.actamat.2011.06.012.

Publisher's Note Springer Nature remains neutral with regard to jurisdictional claims in published maps and institutional affiliations.

Springer Nature or its licensor (e.g. a society or other partner) holds exclusive rights to this article under a publishing agreement with the author(s) or other rightsholder(s); author self-archiving of the accepted manuscript version of this article is solely governed by the terms of such publishing agreement and applicable law.